



THE UNIVERSITY *of* EDINBURGH

Edinburgh Research Explorer

Measurement of the cross-section for electroweak production of dijets in association with a Z boson in pp collisions at $\sqrt{s} = 13$ TeV with the ATLAS detector

Citation for published version:

Clark, PJ, Leonidopoulos, C, Martin, VJ, Mills, C, Collaboration, A, Mijovic, L, Gao, Y & Farrington, S 2017, 'Measurement of the cross-section for electroweak production of dijets in association with a Z boson in pp collisions at $\sqrt{s} = 13$ TeV with the ATLAS detector', *Physics Letters B*, vol. B775, Aaboud:2017emo, pp. 206-228. <https://doi.org/10.1016/j.physletb.2017.10.040>

Digital Object Identifier (DOI):

[10.1016/j.physletb.2017.10.040](https://doi.org/10.1016/j.physletb.2017.10.040)

Link:

[Link to publication record in Edinburgh Research Explorer](#)

Document Version:

Publisher's PDF, also known as Version of record

Published In:

Physics Letters B

General rights

Copyright for the publications made accessible via the Edinburgh Research Explorer is retained by the author(s) and / or other copyright owners and it is a condition of accessing these publications that users recognise and abide by the legal requirements associated with these rights.

Take down policy

The University of Edinburgh has made every reasonable effort to ensure that Edinburgh Research Explorer content complies with UK legislation. If you believe that the public display of this file breaches copyright please contact openaccess@ed.ac.uk providing details, and we will remove access to the work immediately and investigate your claim.





Measurement of the cross-section for electroweak production of dijets in association with a Z boson in pp collisions at $\sqrt{s} = 13$ TeV with the ATLAS detector



The ATLAS Collaboration*

ARTICLE INFO

Article history:

Received 2 October 2017

Received in revised form 19 October 2017

Accepted 19 October 2017

Available online 27 October 2017

Editor: W.-D. Schlatter

ABSTRACT

The cross-section for the production of two jets in association with a leptonically decaying Z boson (Zjj) is measured in proton–proton collisions at a centre-of-mass energy of 13 TeV, using data recorded with the ATLAS detector at the Large Hadron Collider, corresponding to an integrated luminosity of 3.2 fb^{-1} . The electroweak Zjj cross-section is extracted in a fiducial region chosen to enhance the electroweak contribution relative to the dominant Drell–Yan Zjj process, which is constrained using a data-driven approach. The measured fiducial electroweak cross-section is $\sigma_{\text{EW}}^{Zjj} = 119 \pm 16 \text{ (stat.)} \pm 20 \text{ (syst.)} \pm 2 \text{ (lumi.) fb}$ for dijet invariant mass greater than 250 GeV, and $34.2 \pm 5.8 \text{ (stat.)} \pm 5.5 \text{ (syst.)} \pm 0.7 \text{ (lumi.) fb}$ for dijet invariant mass greater than 1 TeV. Standard Model predictions are in agreement with the measurements. The inclusive Zjj cross-section is also measured in six different fiducial regions with varying contributions from electroweak and Drell–Yan Zjj production.

© 2017 The Author(s). Published by Elsevier B.V. This is an open access article under the CC BY license (<http://creativecommons.org/licenses/by/4.0/>). Funded by SCOAP³.

1. Introduction

At the Large Hadron Collider (LHC) events containing a Z boson and at least two jets (Zjj) are produced predominantly via initial-state QCD radiation from the incoming partons in the Drell–Yan process (QCD– Zjj), as shown in Fig. 1(a). In contrast, the production of Zjj events via t -channel electroweak gauge boson exchange (EW– Zjj events), including the vector-boson fusion (VBF) process shown in Fig. 1(b), is a much rarer process. Such VBF processes for vector-boson production are of great interest as a ‘standard candle’ for other VBF processes at the LHC: e.g., the production of Higgs bosons or the search for weakly interacting particles beyond the Standard Model.

The kinematic properties of Zjj events allow some discrimination between the QCD and EW production mechanisms. The emission of a virtual W boson from the quark in EW– Zjj events results in the presence of two high-energy jets, with moderate transverse momentum (p_T), separated by a large interval in rapidity (y)¹ and

therefore with large dijet mass (m_{jj}) that characterises the EW– Zjj signal. A consequence of the exchange of a vector boson in Fig. 1(b) is that there is no colour connection between the hadronic systems produced by the break-up of the two incoming protons. As a result, EW– Zjj events are less likely to contain additional hadronic activity in the rapidity interval between the two high- p_T jets than corresponding QCD– Zjj events.

The first studies of EW– Zjj production were performed [1] in pp collisions at a centre-of-mass energy (\sqrt{s}) of 7 TeV by the CMS Collaboration, where the background-only hypothesis was rejected at the 2.6σ level. The first observation of the EW– Zjj process was performed by the ATLAS Collaboration at a centre-of-mass energy (\sqrt{s}) of 8 TeV [2]. The cross-section measurement is in agreement with predictions from the POWHEG-BOX event generator [3–5] and allowed limits to be placed on anomalous triple gauge couplings. The CMS Collaboration has also observed and measured [6] the cross-section for EW– Zjj production at 8 TeV. This Letter presents measurements of the cross-section for EW– Zjj production and inclusive Zjj production at high dijet invariant mass in pp collisions at $\sqrt{s} = 13$ TeV using data corresponding to an integrated luminosity of 3.2 fb^{-1} collected by the ATLAS detector at the LHC. These measurements allow the dependence of the cross-section on \sqrt{s}

* E-mail address: atlas.publications@cern.ch.

¹ ATLAS uses a right-handed coordinate system with its origin at the nominal interaction point in the centre of the detector and the z -axis along the beam pipe. In the transverse plane, the x -axis points from the interaction point to the centre of the LHC ring, the y -axis points upward, and ϕ is the azimuthal angle around the z -axis. The pseudorapidity is defined in terms of the polar angle θ as $\eta = -\ln \tan(\theta/2)$. The rapidity is defined as $y = 0.5 \ln[(E + p_z)/(E - p_z)]$, where E and p_z are the energy and longitudinal momentum respectively. An angular separation

between two objects is defined as $\Delta R = \sqrt{(\Delta\phi)^2 + (\Delta\eta)^2}$, where $\Delta\phi$ and $\Delta\eta$ are the separations in ϕ and η respectively. Momentum in the transverse plane is denoted by p_T .

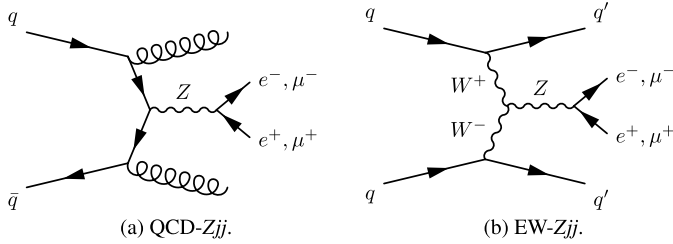


Fig. 1. Examples of leading-order Feynman diagrams for the two production mechanisms for a leptonically decaying Z boson and at least two jets (Zjj) in proton-proton collisions: (a) QCD radiation from the incoming partons (QCD-Zjj) and (b) t -channel exchange of an EW gauge boson (EW-Zjj).

to be studied. The increased \sqrt{s} allows exploration of higher dijet masses, where the EW-Zjj contribution to the total Zjj rate becomes more pronounced.

2. ATLAS detector

The ATLAS detector is described in detail in Refs. [7,8]. It consists of an inner detector for tracking, surrounded by a thin superconducting solenoid, electromagnetic and hadronic calorimeters, and a muon spectrometer incorporating three large superconducting toroidal magnet systems. The inner detector is immersed in a 2 T axial magnetic field and provides charged-particle tracking in the range $|\eta| < 2.5$.

The calorimeters cover the pseudorapidity range $|\eta| < 4.9$. Electromagnetic calorimetry is provided by barrel and end-cap lead/liquid-argon (LAr) calorimeters in the region $|\eta| < 3.2$. Within $|\eta| < 2.47$ the calorimeter is finely segmented in the lateral direction of the showers, allowing measurement of the energy and position of electrons, and providing electron identification in conjunction with the inner detector. Hadronic calorimetry is provided by the steel/scintillator-tile calorimeter, segmented into three barrel structures within $|\eta| < 1.7$, and two hadronic end-cap calorimeters. A copper/LAr hadronic calorimeter covers the $1.5 < |\eta| < 3.2$ region, and a forward copper/tungsten/LAr calorimeter with electromagnetic-shower identification capabilities covers the $3.1 < |\eta| < 4.9$ region.

The muon spectrometer comprises separate trigger and high-precision tracking chambers. The tracking chambers cover the region $|\eta| < 2.7$ with three layers of monitored drift tubes, complemented by cathode strip chambers in part of the forward region, where the hit rate is highest. The muon trigger system covers the range $|\eta| < 2.4$ with resistive plate chambers in the barrel region, and thin gap chambers in the end-cap regions.

A two-level trigger system is used to select events of interest [9]. The Level-1 trigger is implemented in hardware and uses a subset of the detector information to reduce the event rate to around 100 kHz. This is followed by the software-based high-level trigger system which reduces the event rate to about 1 kHz.

3. Monte Carlo samples

The production of EW-Zjj events was simulated at next-to-leading-order (NLO) accuracy in perturbative QCD using the POWHEG-BOX v1 Monte Carlo (MC) event generator [4,5,10] and, alternatively, at leading-order (LO) accuracy in perturbative QCD using the SHERPA 2.2.0 event generator [11]. For modelling of the parton shower, fragmentation, hadronisation and underlying event (UEPS), POWHEG-BOX was interfaced to PYTHIA 8 [12] with a dedicated set of parton-shower-generator parameters (tune) denoted AZNLO [13] and the CT10 NLO parton distribution function (PDF) set [14]. The renormalisation and factorisation scales were set to

the Z boson mass. SHERPA predictions used the COMIX [15] and OPENLOOPS [16] matrix element event generators, and the CKKW method was used to combine the various final-state topologies from the matrix element and match them to the parton shower [17]. The matrix elements were merged with the SHERPA parton shower [18] using the ME+PS@LO prescription [19,20], and using SHERPA's native dynamical scale-setting algorithm to set the renormalisation and factorisation scales. SHERPA predictions used the NNPDF30NNLO PDF set [21].

The production of QCD-Zjj events was simulated using three event generators, SHERPA 2.2.1, ALPGEN 2.14 [22] and MADGRAPH5_aMC@NLO 2.2.2 [23]. SHERPA provides $Z + n$ -parton predictions calculated for up to two partons at NLO accuracy and up to four partons at LO accuracy in perturbative QCD. SHERPA predictions used the NNPDF30NNLO PDF set together with the tuning of the UEPS parameters developed by the SHERPA authors using the ME+PS@NLO prescription [19,20]. ALPGEN is an LO event generator which uses explicit matrix elements for up to five partons and was interfaced to PYTHIA 6.426 [24] using the Perugia2011C tune [25] and the CTEQ6L1 PDF set [26]. Only matrix elements for light-flavour production in ALPGEN are included, with heavy-flavour contributions modelled by the parton shower. MADGRAPH5_aMC@NLO 2.2.2 (MG5_aMC) uses explicit matrix elements for up to four partons at LO, and was interfaced to PYTHIA 8 with the A14 tune [27] and using the NNPDF23LO PDF set [28]. For reconstruction-level studies, total Z boson production rates predicted by all three event generators used to produce QCD-Zjj predictions are normalised using the next-to-next-to-leading-order (NNLO) predictions calculated with the FEWZ 3.1 program [29–31] using the CT10 NNLO PDF set [14]. However, when comparing particle-level theoretical predictions to detector-corrected measurements, the normalisation of quoted predictions is provided by the event generator in question rather than an external NNLO prediction.

The production of a pair of EW vector bosons (diboson), where one decays leptonically and the other hadronically, or where both decay leptonically and are produced in association with two or more jets, through WZ or ZZ production with at least one Z boson decaying to leptons, was simulated separately using SHERPA 2.1.1 and the CT10 NLO PDF set.

The largest background to the selected Zjj samples arises from $t\bar{t}$ and single-top (Wt) production. These were generated using POWHEG-BOX v2 and PYTHIA 6.428 with the Perugia2012 tune [25], and normalised using the cross-section calculated at NNLO+NNLL (next-to-next-to-leading log) accuracy using the Top++2.0 program [32].

All the above MC samples were fully simulated through the GEANT 4 [33] simulation of the ATLAS detector [34]. The effect of additional pp interactions (pile-up) in the same or nearby bunch crossings was also simulated, using PYTHIA v8.186 with the A2 tune [35] and the MSTW2008LO PDF set [36]. The MC samples were reweighted so that the distribution of the average number of pile-up interactions per bunch crossing matches that observed in data. For the data considered in this Letter, the average number of interactions is 13.7.

4. Event preselection

The Z bosons are measured in their dielectron and dimuon decay modes. Candidate events are selected using triggers requiring at least one identified electron or muon with transverse momentum thresholds of $p_T = 24$ GeV and 20 GeV respectively, with additional isolation requirements imposed in these triggers. At higher transverse momenta, the efficiency of selecting candidate events is improved through the use of additional electron and

muon triggers without isolation requirements and with thresholds of $p_T = 60$ GeV and 50 GeV respectively.

Candidate electrons are reconstructed from clusters of energy in the electromagnetic calorimeter matched to inner-detector tracks [37]. They must satisfy the *Medium* identification requirements described in Ref. [37] and have $p_T > 25$ GeV and $|\eta| < 2.47$, excluding the transition region between the barrel and end-cap calorimeters at $1.37 < |\eta| < 1.52$. Candidate muons are identified as tracks in the inner detector matched and combined with track segments in the muon spectrometer. They must satisfy the *Medium* identification requirements described in Ref. [38], and have $p_T > 25$ GeV and $|\eta| < 2.4$. Candidate leptons must also satisfy a set of isolation criteria based on reconstructed tracks and calorimeter activity. Events are required to contain exactly two leptons of the same flavour but of opposite charge. The dilepton invariant mass must satisfy $81 < m_{\ell\ell} < 101$ GeV.

Candidate hadronic jets are required to satisfy $p_T > 25$ GeV and $|y| < 4.4$. They are reconstructed from clusters of energy in the calorimeter [39] using the anti- k_t algorithm [40,41] with radius parameter $R = 0.4$. Jet energies are calibrated by applying p_T - and y -dependent corrections derived from Monte Carlo simulation with additional in situ correction factors determined from data [42]. To reduce the impact of pile-up contributions, all jets with $|y| < 2.4$ and $p_T < 60$ GeV are required to be compatible with having originated from the primary vertex (the vertex with the highest sum of track p_T^2), as defined by the jet vertex tagger algorithm [43]. Selected electrons and muons are discarded if they lie within $\Delta R = 0.4$ of a reconstructed jet. This requirement is imposed to remove non-prompt non-isolated leptons produced in heavy-flavour decays or from the decay in flight of a kaon or pion.

5. Measurement of inclusive Zjj fiducial cross-sections

5.1. Definition of particle-level cross-sections

Cross-sections are measured for inclusive Zjj production that includes the EW- Zjj and QCD- Zjj processes, as well as diboson events. The particle-level production cross-section for inclusive Zjj production in a given fiducial region f is given by

$$\sigma^f = \frac{N_{\text{obs}}^f - N_{\text{bkg}}^f}{L \cdot \mathcal{C}^f}, \quad (1)$$

where N_{obs}^f is the number of events observed in the data passing the selection requirements of the fiducial region under study at detector level, N_{bkg}^f is the corresponding number of expected background (non- Zjj) events, L is the integrated luminosity corresponding to the analysed data sample, and \mathcal{C}^f is a correction factor applied to the observed data yields, which accounts for experimental efficiency and detector resolution effects, and is derived from MC simulation with data-driven efficiency and energy/momentum scale corrections. This correction factor is calculated as:

$$\mathcal{C}^f = \frac{N_{\text{det}}^f}{N_{\text{particle}}^f},$$

where N_{det}^f is the number of signal events that satisfy the fiducial selection criteria at detector level in the MC simulation, and N_{particle}^f is the number of signal events that pass the equivalent selection but at particle level. These correction factors have values between 0.63 and 0.77, depending on the fiducial region.

With the exception of background from multijet and $W +$ jets processes (henceforth referred to together simply as multijet processes), contributions to N_{bkg}^f are estimated using the Monte Carlo

samples described in Section 3. Background from multijet events is estimated from the data by reversing requirements on lepton identification or isolation to derive a template for the contribution of jets mis-reconstructed as lepton candidates as a function of dilepton mass. Non-multijet background is subtracted from the template using simulation. The normalisation is derived by fitting the nominal dilepton mass distribution in each fiducial region with the sum of the multijet template and a template comprising signal and background contributions determined from simulation. The multijet contribution is found to be less than 0.3% in each fiducial region. The contribution from $W +$ jets processes was checked using MC simulation and found to be much smaller than the total multijet background as determined from data.

At particle level, only final-state particles with proper lifetime $c\tau > 10$ mm are considered. Prompt leptons are dressed using the four-momentum combination of an electron or muon and all photons (not originating from hadron decays) within a cone of size $\Delta R = 0.1$ centred on the lepton. These dressed leptons are required to satisfy $p_T > 25$ GeV and $|\eta| < 2.47$. Events are required to contain exactly two dressed leptons of the same flavour but of opposite charge, and the dilepton invariant mass must satisfy $81 < m_{\ell\ell} < 101$ GeV. Jets are reconstructed using the anti- k_t algorithm with radius parameter $R = 0.4$. Prompt leptons and the photons used to dress these leptons are not included in the particle-level jet reconstruction. All remaining final-state particles are included in the particle-level jet clustering. Prompt leptons with a separation $\Delta R_{j,\ell} < 0.4$ from any jet are rejected.

The cross-section measurements are performed in the six phase-space regions defined in Table 1. These regions are chosen to have varying contributions from EW- Zjj and QCD- Zjj processes.

5.2. Event selection

Following Ref. [2], events are selected in six detector fiducial regions. As far as possible, these are defined with the same kinematic requirements as the six phase-space regions in which the cross-section is measured (Table 1). This minimises systematic uncertainties in the modelling of the acceptance.

The baseline fiducial region represents an inclusive selection of events containing a leptonically decaying Z boson and at least two jets with $p_T > 45$ GeV, at least one of which satisfies $p_T > 55$ GeV. The two highest- p_T (leading and sub-leading) jets in a given event define the dijet system. The baseline region is dominated by QCD- Zjj events. The requirement of $81 < m_{\ell\ell} < 101$ GeV suppresses other sources of dilepton events, such as $t\bar{t}$ and $Z \rightarrow \tau\tau$, as well as the multijet background.

Because the energy scale of the dijet system is typically higher in events produced by the EW- Zjj process than in those produced by the QCD- Zjj process, two subsets of the baseline region are defined which probe the EW- Zjj contribution in different ways: in the high-mass fiducial region a high value of the invariant mass of the dijet system ($m_{jj} > 1$ TeV) is required, and in the high- p_T fiducial region the minimum p_T of the leading and sub-leading jets is increased to 85 GeV and 75 GeV respectively. The EW- Zjj process typically produces harder jet transverse momenta and results in a harder dijet invariant mass spectrum than the QCD- Zjj process.

Three additional fiducial regions allow the separate contributions from the EW- Zjj and QCD- Zjj processes to be measured. The EW-enriched fiducial region is designed to enhance the EW- Zjj contribution relative to that from QCD- Zjj , particularly at high m_{jj} . The EW-enriched region is derived from the baseline region requiring $m_{jj} > 250$ GeV, a dilepton transverse momentum of $p_T^{\ell\ell} > 20$ GeV, and that the normalised transverse momentum balance between the two leptons and the two highest transverse

Table 1

Summary of the particle-level selection criteria defining the six fiducial regions (see text for details).

	Fiducial region					
Object	Baseline	High-mass	High- p_{T}	EW-enriched	EW-enriched, $m_{jj} > 1 \text{ TeV}$	QCD-enriched
Leptons	$ \eta < 2.47, p_{\text{T}} > 25 \text{ GeV}, \Delta R_{j,\ell} > 0.4$					
Dilepton pair	$81 < m_{\ell\ell} < 101 \text{ GeV}$					
	–			$p_{\text{T}}^{\ell\ell} > 20 \text{ GeV}$		
Jets	$ y < 4.4$					
	$p_{\text{T}}^{j_1} > 55 \text{ GeV}$		$p_{\text{T}}^{j_1} > 85 \text{ GeV}$	$p_{\text{T}}^{j_1} > 55 \text{ GeV}$		
	$p_{\text{T}}^{j_2} > 45 \text{ GeV}$		$p_{\text{T}}^{j_2} > 75 \text{ GeV}$	$p_{\text{T}}^{j_2} > 45 \text{ GeV}$		
Dijet system	–	$m_{jj} > 1 \text{ TeV}$	–	$m_{jj} > 250 \text{ GeV}$	$m_{jj} > 1 \text{ TeV}$	$m_{jj} > 250 \text{ GeV}$
Interval jets	–			$N_{\text{jet}(p_{\text{T}} > 25 \text{ GeV})}^{\text{interval}} = 0$		$N_{\text{jet}(p_{\text{T}} > 25 \text{ GeV})}^{\text{interval}} \geq 1$
Zjj system	–			$p_{\text{T}}^{\text{balance}} < 0.15$		$p_{\text{T}}^{\text{balance},3} < 0.15$

momentum jets satisfy $p_T^{\text{balance}} < 0.15$. The latter quantity is given by

$$p_T^{\text{balance}} = \frac{|\vec{p}_T^{\ell_1} + \vec{p}_T^{\ell_2} + \vec{p}_T^{j_1} + \vec{p}_T^{j_2}|}{|\vec{p}_T^{\ell_1}| + |\vec{p}_T^{\ell_2}| + |\vec{p}_T^{j_1}| + |\vec{p}_T^{j_2}|}, \quad (2)$$

where \vec{p}_T^i is the transverse momentum vector of object i , ℓ_1 and ℓ_2 label the two leptons that define the Z boson candidate, and j_1 and j_2 refer to the leading and sub-leading jets. These requirements help remove events in which the jets arise from pile-up or multiple parton interactions. The requirement on p_T^{balance} also helps suppress events in which the p_T of one or more jets is badly measured and it enhances the EW- Zjj contribution, where the lower probability of additional radiation causes the Z boson and the dijet system to be well balanced. The EW-enriched region requires a veto [44] on any jets with $p_T > 25$ GeV reconstructed within the rapidity interval bounded by the dijet system ($N_{\text{jet}(p_T>25\text{ GeV})}^{\text{interval}} = 0$). A second fiducial region, denoted EW-enriched ($m_{jj} > 1$ TeV), has identical selection criteria, except for a raised m_{jj} threshold of 1 TeV which further enhances the EW- Zjj contribution to the total Zjj signal rate.

In contrast, the QCD-enriched fiducial region is designed to suppress the EW- Zjj contribution relative to QCD- Zjj by requiring at least one jet with $p_T > 25$ GeV to be reconstructed within the rapidity interval bounded by the dijet system ($N_{\text{jet}(p_T>25\text{ GeV})}^{\text{interval}} \geq 1$). In the QCD-enriched region, the definition of the normalised transverse momentum balance is modified from that given in Eq. (2) to include in the calculation of the numerator and denominator the p_T of the highest p_T jet within the rapidity interval bounded by the dijet system ($p_T^{\text{balance},3}$). In all other respects, the kinematic requirements in the EW-enriched region and QCD-enriched region are identical.

5.3. Detector-level results

In the baseline region, 30686 events are selected in the dielectron channel and 36786 events are selected in the dimuon channel. The total observed yields are in agreement with the expected yields within statistical uncertainties in each dilepton channel. The largest deviation across all fiducial regions is a 2σ (statistical) difference between the expected to observed ratio in the electron versus muon channel in the high- p_T region.

The expected composition of the selected data samples in the six Zjj fiducial regions is summarised in Table 2, averaging across the dielectron and dimuon channels as these compositions in the

two dilepton channels are in agreement within statistical uncertainties. The numbers of selected events in data and expectations from total signal plus background estimates are also given for each region. The largest discrepancy between observed and expected yields is seen in the high-mass region, and results from a mismodelling of the m_{jj} spectrum in the QCD- Zjj MC simulations used, which is discussed below and accounted for in the assessment of systematic uncertainties in the measurement.

5.4. Systematic uncertainties in the inclusive Zjj fiducial cross-sections

Experimental systematic uncertainties affect the determination of the C^f correction factor and the background estimates. The dominant systematic uncertainty in the inclusive Zjj fiducial cross-sections arises from the calibration of the jet energy scale and resolution. This uncertainty varies from around 4% in the EW-enriched region to around 12% in the QCD-enriched region. The larger uncertainty in the QCD-enriched region is due to the higher average jet multiplicity (an average of 1.7 additional jets in addition to the leading and sub-leading jets) compared with the EW-enriched region (an average of 0.4 additional jets). Other experimental systematic uncertainties arising from lepton efficiencies related to reconstruction, identification, isolation and trigger, and lepton energy/momentum scale and resolution as well as from the effect of pile-up, amount to a total of around 1–2%, depending on the fiducial region.

The systematic uncertainty arising from the MC modelling of the m_{jj} distribution in the QCD- Zjj and EW- Zjj signal processes is around 3% in the EW-enriched region, around 1% in the QCD-enriched region, 2% in the high-mass region, and below 1% elsewhere. This is assessed by comparing the correction factors obtained by using the different MC event generators listed in Section 3 and by performing a data-driven reweighting of the QCD- Zjj MC sample to describe the m_{jj} distribution of the observed data in a given fiducial region. Additional contributions arise from varying the QCD renormalisation and factorisation scales up and down by a factor of two independently, and from the propagation of uncertainties in the PDF sets. The normalisation of the diboson contribution is varied according to PDF and scale variations in these predictions [45], and results in up to a 0.1% effect on the measured Zjj cross-sections depending on the fiducial region. The uncertainty from varying the normalisation and shape in m_{jj} of the estimated background from top-quark production is at most 1% (in the high-mass region), arising from changes in the extracted Zjj cross-sections when using modified top-quark background MC samples with PDF and scale variations, suppressed or enhanced additional

Table 2

Estimated composition (in percent) of the data samples selected in the six Zjj fiducial regions for the dielectron and dimuon channels combined, using the EW- Zjj sample from POWHEG, and the QCD- Zjj sample from SHERPA (normalised using NNLO predictions for the inclusive Z cross-section calculated with FEWZ). Uncertainties in the sample contributions are statistical only. Also shown are the total expected yields and the total observed yields in each fiducial region. Uncertainties in the total expected yields are statistical (first) and systematic (second), see Section 5.4 for details.

Process	Composition [%]					
	Baseline	High-mass	High- p_T	EW-enriched	EW-enriched, $m_{jj} > 1$ TeV	QCD-enriched
QCD- Zjj	94.2 ± 0.4	86.8 ± 1.6	92.3 ± 0.4	93.4 ± 0.9	72.9 ± 2.1	95.4 ± 0.8
EW- Zjj	$1.5 \pm < 0.1$	10.6 ± 0.2	$2.6 \pm < 0.1$	$4.8 \pm < 0.1$	26.1 ± 0.5	$1.6 \pm < 0.1$
Diboson	$1.6 \pm < 0.1$	1.5 ± 0.7	2.0 ± 0.5	1.0 ± 0.5	0.8 ± 0.4	1.8 ± 0.4
$t\bar{t}$	$2.6 \pm < 0.1$	1.1 ± 0.1	3.1 ± 0.1	$0.7 \pm < 0.1$	0.1 ± 0.1	1.2 ± 0.1
Single- t	< 0.2	< 0.2	< 0.2	< 0.1	< 0.1	< 0.1
Multijet	< 0.3	< 0.3	< 0.3	< 0.3	< 0.3	< 0.3
Total expected	64800 $\pm 130 \pm 5220$	2220 $\pm 20 \pm 200$	21900 $\pm 40 \pm 1210$	11100 $\pm 50 \pm 520$	640 $\pm 10 \pm 40$	7120 $\pm 30 \pm 880$
Total observed	67472	1471	22461	11630	490	6453

radiation (generated with the PERUGIA2012RADHI/Lo tunes [25]), or using an alternative top-quark production sample from MADGRAPH5_aMC@NLO interfaced to HERWIG++ v2.7.1 [23,46].

The systematic uncertainty in the integrated luminosity is 2.1%. This is derived following a methodology similar to that detailed in Ref. [47], from a calibration of the luminosity scale using x - y beam-separation scans performed in June 2015.

5.5. Inclusive Zjj results

The measured cross-sections in the dielectron and dimuon channels are combined and presented here as a weighted average (taking into account total uncertainties) across both channels. These cross-sections are determined using each of the correction factors derived from the six combinations of the three QCD- Zjj (ALPGEN, MG5_aMC, and SHERPA) and two EW- Zjj (POWHEG and SHERPA) MC samples. For a given fiducial region (Table 1) the cross-section averaged over all six variations is presented in Table 3. The envelope of variation between QCD- Zjj and EW- Zjj models is assigned as a source of systematic uncertainty (1% in all regions except the EW-enriched region where the variation is 3% and the high-mass region where the variation is 2%).

The theoretical predictions from SHERPA (QCD- Zjj) + POWHEG (EW- Zjj), MG5_aMC (QCD- Zjj) + POWHEG (EW- Zjj), and ALPGEN (QCD- Zjj) + POWHEG (EW- Zjj) are found to be in agreement with the measurements in most cases. The uncertainties in the theoretical predictions are significantly larger than the uncertainties in the corresponding measurements.

The largest differences between predictions and measurement are in the high-mass and EW-enriched ($m_{jj} > 250$ GeV and > 1 TeV) regions. Predictions from SHERPA (QCD- Zjj) + POWHEG (EW- Zjj) and MG5_aMC (QCD- Zjj) + POWHEG (EW- Zjj) exceed measurements in the high-mass region by 54% and 34% respectively, where the predictions have relative uncertainties with respect to the measurement of 36% and 32%. For the EW-enriched region, SHERPA (QCD- Zjj) + POWHEG (EW- Zjj) describes the observed rates well, but MG5_aMC (QCD- Zjj) + POWHEG (EW- Zjj) overestimates measurements by 28% with a relative uncertainty of 11%. In the EW-enriched ($m_{jj} > 1$ TeV) region the same predictions overestimate measured rates by 33% and 57%, with relative uncertainties of 16% and 15%. Some of these differences arise from a significant mismodelling of the QCD- Zjj contribution, as investigated and discussed in detail in Section 6.1. Predictions from

ALPGEN (QCD- Zjj) + POWHEG (EW- Zjj) are in agreement with the data for the high-mass and EW-enriched ($m_{jj} > 250$ GeV and > 1 TeV) regions.

6. Measurement of EW- Zjj fiducial cross-sections

The EW-enriched fiducial region (defined in Table 1) is used to measure the production cross-section of the EW- Zjj process. The EW-enriched region has an overall expected EW- Zjj signal fraction of 4.8% (Table 2) and this signal fraction grows with increasing m_{jj} to 26.1% for $m_{jj} > 1$ TeV. The QCD-enriched region has an overall expected EW- Zjj signal fraction of 1.6% increasing to 4.4% for $m_{jj} > 1$ TeV. The dominant background to the EW- Zjj cross-section measurement is QCD- Zjj production. It is subtracted in the same way as non- Zjj backgrounds in the inclusive measurement described in Section 5. Although diboson production includes contributions from purely EW processes, in this measurement it is considered as part of the background and is estimated from simulation.

A particle-level production cross-section measurement of EW- Zjj production in a given fiducial region f is thus given by

$$\sigma_{EW}^f = \frac{N_{obs}^f - N_{QCD-Zjj}^f - N_{bkg}^f}{L \cdot \mathcal{C}_{EW}^f}, \quad (3)$$

with the same notations as in Eq. (1) and where $N_{QCD-Zjj}^f$ is the expected number of QCD- Zjj events passing the selection requirements of the fiducial region at detector level, N_{bkg}^f is the expected number of background (non- Zjj and diboson) events, and \mathcal{C}_{EW}^f is a correction factor applied to the observed background-subtracted data yields that accounts for experimental efficiency and detector resolution effects, and is derived from EW- Zjj MC simulation with data-driven efficiency and energy/momentum scale corrections. For the $m_{jj} > 250$ GeV ($m_{jj} > 1$ TeV) region this correction factor is determined to be 0.66 (0.67) when using the SHERPA EW- Zjj prediction, and 0.67 (0.68) when using the POWHEG EW- Zjj prediction.

Detector-level comparisons of the m_{jj} distribution between data and simulation in (a) the EW-enriched region and (b) the QCD-enriched region are shown in Fig. 2. It can be seen in Fig. 2(a)

Table 3

Measured and predicted inclusive Zjj production cross-sections in the six fiducial regions defined in Table 1. For the measured cross-sections, the first uncertainty given is statistical, the second is systematic and the third is due to the luminosity determination. For the predictions, the statistical uncertainty is added in quadrature to the systematic uncertainties arising from the PDFs and factorisation and renormalisation scale variations.

Fiducial region	Inclusive Zjj cross-sections [pb]						
	Measured				Prediction		
	value	\pm stat.	\pm syst.	\pm lumi.	SHERPA (QCD- Zjj) +PowHEG (EW- Zjj)	MG5_aMC (QCD- Zjj) +PowHEG (EW- Zjj)	ALPGEN (QCD- Zjj) +PowHEG (EW- Zjj)
Baseline	13.9	± 0.1	± 1.1	± 0.3	13.5 ± 1.9	15.2 ± 2.2	11.7 ± 1.7
High- p_T	4.77	± 0.05	± 0.27	± 0.10	4.7 ± 0.8	5.5 ± 0.9	4.2 ± 0.7
EW-enriched	2.77	± 0.04	± 0.13	± 0.06	2.7 ± 0.2	3.6 ± 0.3	2.4 ± 0.2
QCD-enriched	1.34	± 0.02	± 0.17	± 0.03	1.5 ± 0.4	1.4 ± 0.3	1.1 ± 0.3
High-mass	0.30	± 0.01	± 0.03	± 0.01	0.46 ± 0.11	0.40 ± 0.09	0.27 ± 0.06
EW-enriched ($m_{jj} > 1$ TeV)	0.118	± 0.008	± 0.006	± 0.002	0.156 ± 0.019	0.185 ± 0.023	0.120 ± 0.015

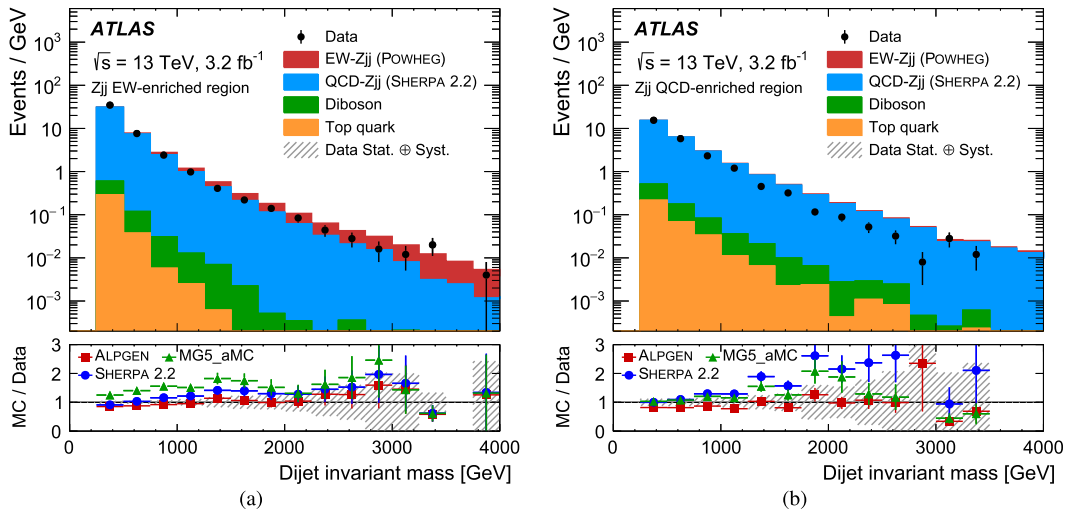


Fig. 2. Detector-level comparisons of the dijet invariant mass distribution between data and simulation in (a) the EW-enriched region and (b) the QCD-enriched region, for the dielectron and dimuon channel combined. Uncertainties shown on the data are statistical only. The EW- Zjj simulation sample comes from the PowHEG event generator and the QCD- Zjj MC sample comes from the SHERPA event generator. The lower panels show the ratio of simulation to data for three QCD- Zjj models, from ALPGEN, MG5_aMC, and SHERPA. The hatched band centred at unity represents the size of statistical and experimental systematic uncertainties added in quadrature.

that in the EW-enriched region the EW- Zjj component becomes prominent at large values of m_{jj} . However, Fig. 2(b) demonstrates that the shape of the m_{jj} distribution for QCD- Zjj production is poorly modelled in simulation. The same trend is seen for all three QCD- Zjj event generators listed in Section 3. ALPGEN provides the best description of the data over the whole m_{jj} range. In comparison, MG5_aMC and SHERPA overestimate the data by 80% and 120% respectively, for $m_{jj} = 2$ TeV, well outside the uncertainties on these predictions described in Table 3. These discrepancies have been observed previously in Zjj [2,48] and Wjj [49–51] production at high dijet invariant mass and at high jet rapidities. For the purpose of extracting the cross-section for EW- Zjj production, this mismodelling of QCD- Zjj is corrected for using a data-driven approach, as discussed in the following.

6.1. Corrections for mismodelling of QCD- Zjj production and fitting procedure

The normalisation of the QCD- Zjj background is extracted from a fit of the QCD- Zjj and EW- Zjj m_{jj} simulated distributions to the data in the EW-enriched region, after subtraction of non- Zjj and diboson background, using a log-likelihood maximisation [52]. Following the procedure adopted in Ref. [2], the data in the QCD-

enriched region are used to evaluate detector-level shape correction factors for the QCD- Zjj MC predictions bin-by-bin in m_{jj} . These data-to-simulation ratio correction factors are applied to the simulation-predicted shape in m_{jj} of the QCD- Zjj contribution in the EW-enriched region. This procedure is motivated by two observations:

- the QCD-enriched region and EW-enriched region are designed to be kinematically very similar, differing only with regard to the presence/absence of jets reconstructed within the rapidity interval bounded by the dijet system,
- the contribution of EW- Zjj to the region of high m_{jj} is suppressed in the QCD-enriched region (4.4% for $m_{jj} > 1$ TeV) relative to that in the EW-enriched region (26.1% for $m_{jj} > 1$ TeV) (also illustrated in Fig. 2); the impact of the residual EW- Zjj contamination in the QCD-enriched region is assigned as a component of the systematic uncertainty in the QCD- Zjj background.

The shape correction factors in m_{jj} obtained using the three different QCD- Zjj MC samples are shown in Fig. 3(a). These are derived as the ratio of the data to simulation in bins of m_{jj} after normalisation of the total yield in simulation to that observed

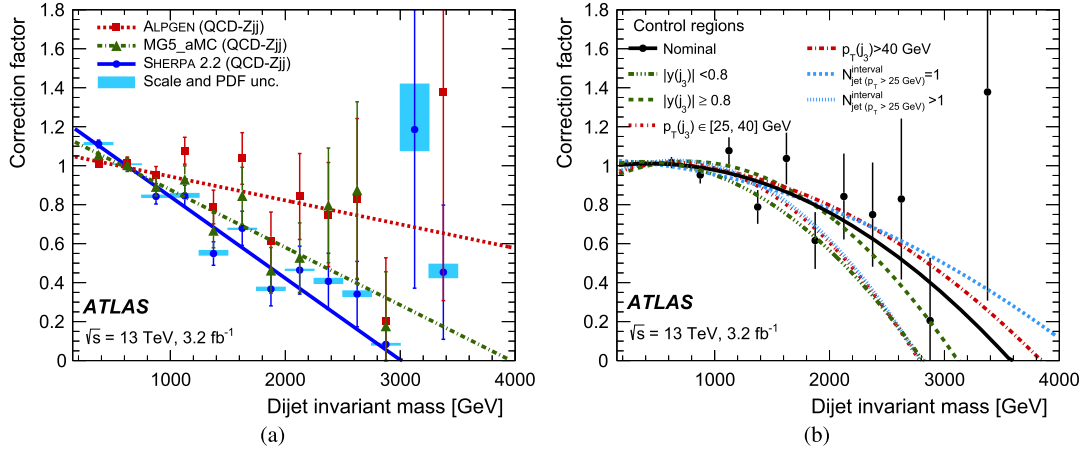


Fig. 3. Binned data-to-simulation normalised ratio shape correction factors as a function of dijet invariant mass in the QCD-enriched region. (a) Ratio for three different QCD-Zjj MC samples with uncertainties corresponding to the combined statistical uncertainties in the data and QCD-Zjj MC samples added in quadrature. Scale and PDF uncertainties in SHERPA predictions are indicated by the shaded bands. Lines represent fits to the ratios using a linear fit. (b) Ratio for subregions of the QCD-enriched region for the ALPGEN MC sample. Curves represent the result of fits with a quadratic function for the various subregions.

in data in the QCD-enriched region. A binned fit to the correction factors derived in dijet invariant mass is performed with a linear fit function (and also with a quadratic fit function) to produce a continuous correction factor. The linear fit is illustrated overlaid on the binned correction factors in Fig. 3(a). The nominal value of the EW-Zjj cross-section corresponding to a particular QCD-Zjj event generator template is determined using the correction factors from the linear fit. The change in resultant EW-Zjj cross-section from using binned correction factors directly is assessed as a systematic uncertainty. The change in the extracted EW-Zjj cross-section when using a quadratic fit was found to be negligible. The variations observed between event generators may be partly due to differences in the modelling of QCD radiation within the rapidity interval bounded by the dijet system, which affects the extrapolation from the central-jet-enriched QCD-enriched region to the central-jet-suppressed EW-enriched region. The variation between event generators is much larger than the effect of PDF and scale uncertainties in a particular prediction (indicated in Fig. 3(a) by a shaded band on the predictions from SHERPA). Estimating the uncertainties associated with QCD-Zjj mismodelling from PDF and scale variations around a single generator prediction would thus result in an underestimate of the true theoretical uncertainty associated with this mismodelling. In this measurement, the span of resultant EW-Zjj cross-sections extracted from the use of each of the three QCD-Zjj templates is assessed as a systematic uncertainty. The variation in the EW-Zjj cross-section measurement due to a change in the EW-Zjj signal template used in the derivation of the m_{jj} correction factors (from POWHEG to SHERPA) is found to be negligible.

To test the dependence of the QCD-Zjj correction factors on the modelling of any additional jet emitted in the dijet rapidity interval, the QCD-enriched control region is divided into pairs of mutually exclusive subsets according to the $|y|$ of the highest p_T jet within the rapidity interval bounded by the dijet system, the p_T of that jet, or the value of $N_{\text{jet}}^{\text{interval}}(p_T > 25 \text{ GeV})$. The continuous correction factors are determined from each subregion using both a linear and a quadratic fit to the data. Correction factors derived in the subregions using quadratic fits result in the largest variation in the extracted cross-sections. These fits are shown in Fig. 3(b) for the ALPGEN QCD-Zjj sample, which displays the largest variation between subregions of the three event generators used to produce QCD-Zjj predictions. Within statistical uncertainties the measured EW-Zjj cross-sections are not sensitive to the definition of the control region used.

The normalisations of the corrected QCD-Zjj templates and the EW-Zjj templates are allowed to vary independently in a fit to the background-subtracted m_{jj} distribution in the EW-enriched region. The measured electroweak production cross-section is determined from the data minus the QCD-Zjj contribution determined from these fits (Eq. (3)). As the choice of EW-Zjj template can influence the normalisation of the QCD-Zjj template in the EW-enriched region fit, the measured EW-Zjj cross-section determination is repeated for each QCD-Zjj template using either the POWHEG or SHERPA EW-Zjj template in the fit. The central value of the result quoted is the average of the measured EW-Zjj cross-sections determined with each of the six combinations of the three QCD-Zjj and two EW-Zjj templates, with the envelope of measured results from these variations taken as an uncertainty associated with the dependence on the modelling of the templates in the EW-enriched region. Separate uncertainties are assigned for the determination of the QCD-Zjj correction factors in the QCD-enriched region and their propagation into the EW-enriched region. The measurement of the EW-Zjj cross-section in the EW-enriched region for $m_{jj} > 1$ TeV is extracted from the same fit procedure, with data and QCD-Zjj yields integrated for $m_{jj} > 1$ TeV.

Fig. 4(a) shows a comparison in the EW-enriched region of the fitted EW-Zjj and m_{jj} -reweighted QCD-Zjj templates to the background-subtracted data, from which the measured EW-Zjj cross-section is extracted. Fig. 4(b) demonstrates how the data in the EW-enriched region is modelled with the fitted EW-Zjj and m_{jj} -reweighted QCD-Zjj templates, for the three different QCD-Zjj event generators (and their corresponding correction factors derived in the QCD-enriched region shown in Fig. 3(a)). Despite significantly different modelling of the m_{jj} distribution between event generators, and different models for additional QCD radiation, the results of the combined correction and fit procedure give a consistent description of the data.

6.2. Systematic uncertainties in the EW-Zjj fiducial cross-section

The total systematic uncertainty in the cross-section for EW-Zjj production in the EW-enriched fiducial region is 17% (16% in the EW-enriched $m_{jj} > 1$ TeV region). The sources and size of each systematic uncertainty are summarised in Table 4.

Systematic uncertainties associated with the EW-Zjj signal template used in the fit and EW-Zjj signal extraction are obtained from the variation in the measured cross-section when using either of the individual EW-Zjj MC samples (POWHEG and SHERPA)

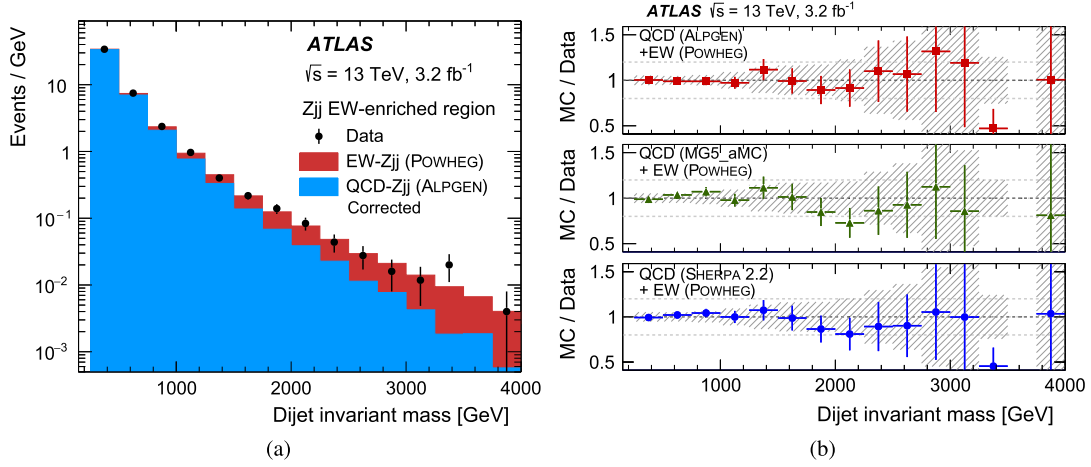


Fig. 4. (a) Comparison in the EW-enriched region of the sum of EW-Zjj and m_{jj} -reweighted QCD-Zjj templates to the data (minus the non-Zjj backgrounds). The normalisation of the templates is adjusted to the results of the fit (see text for details). The EW-Zjj MC sample comes from the POWHEG event generator and the QCD-Zjj MC sample comes from the ALPGEN event generator. (b) The ratio of the sum of the EW-Zjj and m_{jj} -reweighted QCD-Zjj templates to the background-subtracted data in the EW-enriched region, for three different QCD-Zjj MC predictions. The normalisation of the templates is adjusted to the results of the fit. Error bars represent the statistical uncertainties in the data and combined QCD-Zjj plus EW-Zjj MC samples added in quadrature. The hatched band represents experimental systematic uncertainties in the m_{jj} distribution.

Table 4

Systematic uncertainties contributing to the measurement of the EW-Zjj cross-sections for $m_{jj} > 250$ GeV and $m_{jj} > 1$ TeV. Uncertainties are grouped into EW-Zjj signal modelling, QCD-Zjj background modelling, QCD-EW interference, non-Zjj backgrounds, and experimental sources.

Source	Relative systematic uncertainty [%]	
	$\sigma_{EW}^{m_{jj} > 250 \text{ GeV}}$	$\sigma_{EW}^{m_{jj} > 1 \text{ TeV}}$
EW-Zjj signal modelling (QCD scales, PDF and UEPS)	± 7.4	± 1.7
EW-Zjj template statistical uncertainty	± 0.5	± 0.04
<hr/>		
EW-Zjj contamination in QCD-enriched region	-0.1	-0.2
QCD-Zjj modelling (m_{jj} shape constraint / third-jet veto)	± 11	± 11
Stat. uncertainty in QCD control region constraint	± 6.2	± 6.4
QCD-Zjj signal modelling (QCD scales, PDF and UEPS)	± 4.5	± 6.5
QCD-Zjj template statistical uncertainty	± 2.5	± 3.5
<hr/>		
QCD-EW interference	± 1.3	± 1.5
<hr/>		
$t\bar{t}$ and single-top background modelling	± 1.0	± 1.2
Diboson background modelling	± 0.1	± 0.1
<hr/>		
Jet energy resolution	± 2.3	± 1.1
Jet energy scale	+5.3/-4.1	+3.5/-4.2
Lepton identification, momentum scale, trigger, pile-up	+1.3/-2.5	+3.2/-1.5
Luminosity	± 2.1	± 2.1
Total	± 17	± 16

compared to the average of the two, taken as the central value. Uncertainties in the EW-Zjj templates due to variations of the QCD scales, of the PDFs, and of the UEPS model are also included as are statistical uncertainties in the templates themselves.

Following the extraction of the EW-Zjj cross-section in the EW-enriched regions, the normalisations of the EW-Zjj MC samples are modified to agree with the measurements and the potential EW contamination of the QCD-enriched region is recalculated, which leads to a modification of the QCD-Zjj correction factors. The EW-Zjj cross-section measurement is repeated with these modified QCD-Zjj templates and the change in the resultant cross-sections is assigned as a systematic uncertainty associated with the EW-Zjj contamination of the QCD-enriched region.

As discussed in Section 6.1, the use of a QCD-enriched region provides a way to correct for QCD-Zjj modelling issues and also constrains theoretical and experimental uncertainties associated with observables constructed from the two leading jets. Neverthe-

less, the largest contribution to the total uncertainty arises from modelling uncertainties associated with propagation of the m_{jj} correction factors for QCD-Zjj in the QCD-enriched region into the EW-enriched region, and these correction factors depend on the modelling of the additional jet activity in the QCD-Zjj MC samples used in the measurement. The uncertainty is assessed by repeating the EW-Zjj cross-section measurement with m_{jj} -reweighted QCD-Zjj MC templates from ALPGEN, MG5_aMC, and SHERPA, and assigning the variation of the measured cross-sections from the central EW-Zjj result as a systematic uncertainty. Statistical uncertainties from data and simulation in the m_{jj} correction factors derived in the QCD-enriched region are also propagated through to the measured EW-Zjj cross-section as a systematic uncertainty. Uncertainties associated with QCD renormalisation and factorisation scales, PDF error sets, and UEPS modelling are assessed by studying the change in the extracted EW-Zjj cross-sections when repeating the measurement procedure, including rederiving

m_{jj} correction factors in the QCD-enriched region and repeating fits in the EW-enriched region, using modified QCD- Zjj MC templates. Statistical uncertainties in the QCD- Zjj template in the EW-enriched region are also propagated as a systematic uncertainty in the EW- Zjj cross-section measurement.

Potential quantum-mechanical interference between the QCD- Zjj and EW- Zjj processes is assessed using MG5_aMC to derive a correction to the QCD- Zjj template as a function of m_{jj} . The impact of interference on the measurement is determined by repeating the EW- Zjj measurement procedure twice, either applying this correction to the QCD- Zjj template only in the QCD-enriched region or only in the EW-enriched region and taking the maximum change in the measured EW- Zjj cross-section as a symmetrised uncertainty. This approach assumes the interference affects only one of the two fiducial regions and therefore has a maximal impact on the signal extraction. Potential interference between the Zjj and diboson processes was found to be negligible.

Normalisation and shape uncertainties in the estimated background from top-quark and diboson production are assessed with varied background templates as described in Section 5.4, albeit with significantly larger uncertainties in the EW-enriched fiducial region compared to the baseline region.

Experimental systematic uncertainties arising from the jet energy scale and resolution, from lepton efficiencies related to reconstruction, identification, isolation and trigger, and lepton energy/momentum scale and resolution, and from pile-up modelling, are independently assessed by repeating the EW- Zjj measurement procedure using modified QCD- Zjj and EW- Zjj templates. Here, the QCD-enriched QCD- Zjj template constraint procedure described in Section 6.1 has the added benefit of significantly reducing the jet-based experimental uncertainties, as can be seen in Table 4 from their small impact on the total systematic uncertainty.

6.3. Electroweak Zjj results

As in the inclusive Zjj cross-section measurements, the quoted EW- Zjj cross-section measurements are the average of the cross-sections determined with each of the six combinations of the three QCD- Zjj MC templates and two EW- Zjj MC templates. The measured cross-sections for the EW production of a leptonically decaying Z boson and at least two jets satisfying the fiducial requirements for the EW-enriched regions as given in Table 1 with the requirements $m_{jj} > 250$ GeV and $m_{jj} > 1$ TeV are shown in Table 5, where they are compared to predictions from POWHEG+PYTHIA. The use of a differential template fit in m_{jj} to extract the EW- Zjj signal allows systematic uncertainties on the EW- Zjj cross-section measurements to be constrained by the bins with the most favourable balance of EW- Zjj signal purity and minimal shape and normalisation uncertainty. For the $m_{jj} > 250$ GeV region, although all m_{jj} bins contribute to the fit, the individually most-constraining m_{jj} interval is the 900–1000 GeV bin. The use of this method results in very similar relative systematic uncertainties in the EW- Zjj cross-section measurements at the two different m_{jj} thresholds, despite the measured relative EW- Zjj contribution to the total Zjj rate for $m_{jj} > 1$ TeV being more than six times the relative contribution of EW- Zjj for $m_{jj} > 250$ GeV.

The EW- Zjj cross-sections at $\sqrt{s} = 13$ TeV are in agreement with the predictions from POWHEG+PYTHIA for both $m_{jj} > 250$ GeV and $m_{jj} > 1$ TeV. The effect on the measurement of inclusive Zjj production rates (Section 5.5) from correcting the EW- Zjj production rates predicted by POWHEG+PYTHIA to the measured rates presented here was found to be negligible. Modifications to the m_{jj} distribution shape are already accounted for as a systematic uncertainty in the inclusive Zjj measurements.

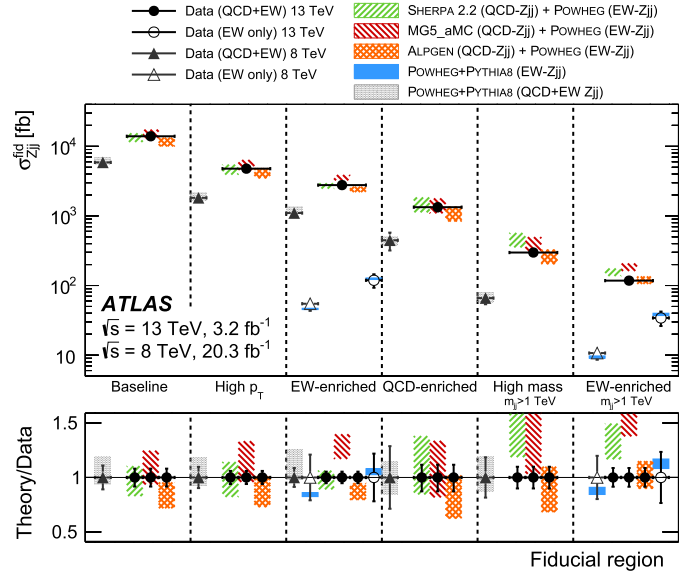


Fig. 5. Fiducial cross-sections for a leptonically decaying Z boson and at least two jets (solid data points) and EW- Zjj production (open data points) at 13 TeV (circles) compared to equivalent results at 8 TeV [2] (triangles) and to theoretical predictions (shaded/hatched bands). Measurements of Zjj at 13 TeV are compared to predictions from SHERPA (QCD- Zjj) + POWHEG (EW- Zjj), MG5_aMC (QCD- Zjj) + POWHEG (EW- Zjj), and ALPGEN (QCD- Zjj) + POWHEG (EW- Zjj), while measurements of EW- Zjj production are compared to POWHEG (EW- Zjj). Results at 8 TeV are compared to predictions from POWHEG+PYTHIA (QCD- Zjj + EW- Zjj). The bottom panel shows the ratio of the various theory predictions to data as shaded bands. Relative uncertainties in the measured data are represented by an error bar centred at unity.

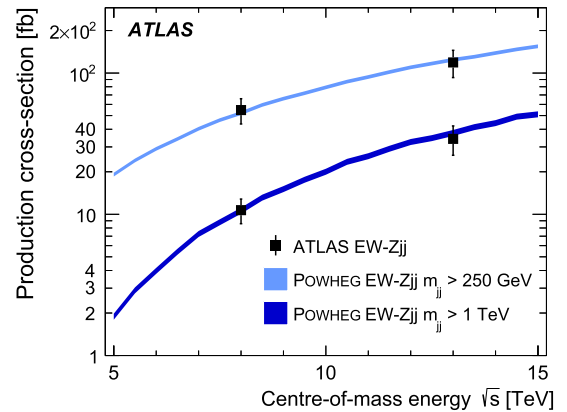


Fig. 6. Measurements of the EW- Zjj process presented in this Letter at a centre-of-mass energy of 13 TeV, compared with previous measurements at 8 TeV [2], for two different dijet invariant mass thresholds, $m_{jj} > 0.25$ TeV and $m_{jj} > 1$ TeV. The error bars on the measurements represent statistical and systematic uncertainties added in quadrature. Predictions from the POWHEG event generator with their total uncertainty are also shown.

Fig. 5 shows a summary of the fiducial cross-sections for a leptonically decaying Z boson and at least two jets at 13 TeV compared to equivalent results at 8 TeV [2] and to theoretical predictions with their uncertainties. A significant rise in cross-section is observed between $\sqrt{s} = 8$ TeV and $\sqrt{s} = 13$ TeV within each fiducial region. In the EW-enriched region, for m_{jj} thresholds of 250 GeV and 1 TeV, the measured EW- Zjj cross-sections at 13 TeV are found to be respectively 2.2 and 3.2 times as large as those measured at 8 TeV, as illustrated in Fig. 6.

Table 5

Measured and predicted EW- Zjj production cross-sections in the EW-enriched fiducial regions with and without an additional kinematic requirement of $m_{jj} > 1$ TeV. For the measured cross-sections, the first uncertainty given is statistical, the second is systematic and the third is due to the luminosity determination. For the predictions, the quoted uncertainty represents the statistical uncertainty, plus systematic uncertainties from the PDFs and factorisation and renormalisation scale variations, all added in quadrature.

Fiducial region	EW- Zjj cross-sections [fb]				
	Measured		POWHEG+PYTHIA		
EW-enriched, $m_{jj} > 250$ GeV	119	± 16	± 20	± 2	125.2 ± 3.4
EW-enriched, $m_{jj} > 1$ TeV	34.2	± 5.8	± 5.5	± 0.7	38.5 ± 1.5

7. Summary

Fiducial cross-sections for the electroweak production of two jets in association with a leptonically decaying Z boson in proton–proton collisions are measured at a centre-of-mass energy of 13 TeV, using data corresponding to an integrated luminosity of 3.2 fb^{-1} recorded with the ATLAS detector at the Large Hadron Collider. The EW- Zjj cross-section is extracted in a fiducial region chosen to enhance the EW contribution relative to the dominant QCD- Zjj process, which is constrained using a data-driven approach. The measured fiducial EW cross-section is $\sigma_{EW}^{Zjj} = 119 \pm 16$ (stat.) ± 20 (syst.) ± 2 (lumi.) fb for dijet invariant mass greater than 250 GeV, and 34.2 ± 5.8 (stat.) ± 5.5 (syst.) ± 0.7 (lumi.) fb for dijet invariant mass greater than 1 TeV. A comparison with previously published measurements at $\sqrt{s} = 8$ TeV is presented, with measured EW- Zjj cross-sections at $\sqrt{s} = 13$ TeV found to be 2.2 (3.2) times as large as those measured at $\sqrt{s} = 8$ TeV in the low (high) dijet mass EW-enriched regions. Relative to measurements at $\sqrt{s} = 8$ TeV, the increased \sqrt{s} allows a region of higher dijet mass to be explored, in which the EW- Zjj signal is more prominent. The Standard Model predictions are in agreement with the EW- Zjj measurements.

The inclusive Zjj cross-section is also measured in six different fiducial regions with varying contributions from EW- Zjj and QCD- Zjj production. At higher dijet invariant masses (> 1 TeV), particularly crucial for precision measurements of EW- Zjj production and for searches for new phenomena in vector-boson fusion topologies, predictions from SHERPA (QCD- Zjj) + POWHEG (EW- Zjj) and MG5_aMC (QCD- Zjj) + POWHEG (EW- Zjj) are found to significantly overestimate the observed Zjj production rates in data. ALPGEN (QCD- Zjj) + POWHEG (EW- Zjj) provides a better description of the m_{jj} shape.

Acknowledgements

We thank CERN for the very successful operation of the LHC, as well as the support staff from our institutions without whom ATLAS could not be operated efficiently.

We acknowledge the support of ANPCyT, Argentina; YerPhI, Armenia; ARC, Australia; BMWFW and FWF, Austria; ANAS, Azerbaijan; SSTC, Belarus; CNPq and FAPESP, Brazil; NSERC, NRC and CFI, Canada; CERN; CONICYT, Chile; CAS, MOST and NSFC, China; COLCIENCIAS, Colombia; MSMT CR, MPO CR and VSC CR, Czech Republic; DNRF and DNSRC, Denmark; IN2P3-CNRS, CEA-DSM/IRFU, France; SRNSF, Georgia; BMBF, HGF, and MPG, Germany; GSRT, Greece; RGC, Hong Kong SAR, China; ISF, I-CORE and Benoziyo Center, Israel; INFN, Italy; MEXT and JSPS, Japan; CNRST, Morocco; NWO, Netherlands; RCN, Norway; MNiSW and NCN, Poland; FCT, Portugal; MNE/IFA, Romania; MES of Russia and NRC KI, Russian Federation; JINR; MESTD, Serbia; MSSR, Slovakia; ARRS and MIZŠ, Slovenia; DST/NRF, South Africa; MINECO, Spain; SRC and Knut and Alice Wallenberg Foundation, Sweden; SERI, SNSF and Cantons of Bern and Geneva, Switzerland; MOST, Taiwan; TAEK, Turkey; STFC,

United Kingdom; DOE and NSF, United States of America. In addition, individual groups and members have received support from BCKDF, the Canada Council, Canarie, CRC, Compute Canada, FQRNT, and the Ontario Innovation Trust, Canada; EPLANET, ERC, ERDF, FP7, Horizon 2020 and Marie Skłodowska-Curie Actions, European Union; Investissements d’Avenir Labex and Idex, ANR, Région Auvergne and Fondation Partager le Savoir, France; DFG and AvH Foundation, Germany; Herakleitos, Thales and Aristeia programmes co-financed by EU-ESF and the Greek NSRF; BSF, GIF and Minerva, Israel; BRF, Norway; CERCA Programme Generalitat de Catalunya, Generalitat Valenciana, Spain; the Royal Society and Leverhulme Trust, United Kingdom.

The crucial computing support from all WLCG partners is acknowledged gratefully, in particular from CERN, the ATLAS Tier-1 facilities at TRIUMF (Canada), NDGF (Denmark, Norway, Sweden), CC-IN2P3 (France), KIT/GridKA (Germany), INFN-CNAF (Italy), NL-T1 (Netherlands), PIC (Spain), ASGC (Taiwan), RAL (UK) and BNL (USA), the Tier-2 facilities worldwide and large non-WLCG resource providers. Major contributors of computing resources are listed in Ref. [53].

References

- [1] CMS Collaboration, Measurement of the hadronic activity in events with a Z and two jets and extraction of the cross section for the electroweak production of a Z with two jets in pp collisions at $\sqrt{s} = 7$ TeV, J. High Energy Phys. 10 (2013) 062, arXiv:1305.7389 [hep-ex].
- [2] ATLAS Collaboration, Measurement of the electroweak production of dijets in association with a Z -boson and distributions sensitive to vector boson fusion in proton–proton collisions at $\sqrt{s} = 8$ TeV using the ATLAS detector, J. High Energy Phys. 04 (2014) 031, arXiv:1401.7610 [hep-ex].
- [3] P. Nason, A new method for combining NLO QCD with shower Monte Carlo algorithms, J. High Energy Phys. 11 (2004) 040, arXiv:hep-ph/0409146.
- [4] S. Frixione, P. Nason, C. Oleari, Matching NLO QCD computations with Parton Shower simulations: the POWHEG method, J. High Energy Phys. 11 (2007) 070, arXiv:0709.2092 [hep-ph].
- [5] S. Alioli, et al., A general framework for implementing NLO calculations in shower Monte Carlo programs: the POWHEG BOX, J. High Energy Phys. 06 (2010) 043, arXiv:1002.2581 [hep-ph].
- [6] CMS Collaboration, Measurement of electroweak production of two jets in association with a Z boson in proton–proton collisions at $\sqrt{s} = 8$ TeV, Eur. Phys. J. C 75 (2015) 66, arXiv:1410.3153 [hep-ex].
- [7] ATLAS Collaboration, The ATLAS experiment at the CERN Large Hadron Collider, J. Instrum. 3 (2008) S08003.
- [8] ATLAS Collaboration, ATLAS Insertable B-Layer, Technical Design Report, ATLAS-TDR-19, 2010, <https://cds.cern.ch/record/1291633>; ATLAS Insertable B-Layer, Technical Design Report Addendum, ATLAS-TDR-19-ADD-1, <https://cds.cern.ch/record/1451888>, 2012.
- [9] ATLAS Collaboration, Performance of the ATLAS trigger system in 2015, Eur. Phys. J. C 77 (2017) 317, arXiv:1611.09661 [hep-ex].
- [10] F. Schissler, D. Zeppenfeld, Parton shower effects on W and Z production via vector boson fusion at NLO QCD, J. High Energy Phys. 04 (2013) 057, arXiv:1302.2884 [hep-ph].
- [11] T. Gleisberg, et al., Event generation with SHERPA 1.1, J. High Energy Phys. 02 (2009) 007, arXiv:0811.4622 [hep-ph].
- [12] T. Sjöstrand, et al., An introduction to PYTHIA 8.2, Comput. Phys. Commun. 191 (2015) 159, arXiv:1410.3012 [hep-ph].
- [13] ATLAS Collaboration, Measurement of the Z/γ^* boson transverse momentum distribution in pp collisions at $\sqrt{s} = 7$ TeV with the ATLAS detector, J. High Energy Phys. 09 (2014) 145, arXiv:1406.3660 [hep-ex].

- [14] H.-L. Lai, et al., New parton distributions for collider physics, *Phys. Rev. D* 82 (2010) 074024, arXiv:1007.2241 [hep-ph].
- [15] T. Gleisberg, S. Höche, Comix, a new matrix element generator, *J. High Energy Phys.* 12 (2008) 039, arXiv:0808.3674 [hep-ph].
- [16] F. Cascioli, P. Maierhöfer, S. Pozzorini, Scattering amplitudes with open loops, *Phys. Rev. Lett.* 108 (2012) 111601, arXiv:1111.5206 [hep-ph].
- [17] S. Catani, et al., QCD matrix elements + parton showers, *J. High Energy Phys.* 11 (2001) 063, arXiv:hep-ph/0109231.
- [18] S. Schumann, F. Krauss, A parton shower algorithm based on Catani–Seymour dipole factorisation, *J. High Energy Phys.* 03 (2008) 038, arXiv:0709.1027 [hep-ph].
- [19] T. Gehrmann, S. Hoche, F. Krauss, M. Schonherr, F. Siegert, NLO QCD matrix elements + parton showers in $e^+e^- \rightarrow \text{hadrons}$, *J. High Energy Phys.* 01 (2013) 144, arXiv:1207.5031 [hep-ph].
- [20] S. Höche, et al., QCD matrix elements + parton showers: the NLO case, *J. High Energy Phys.* 04 (2013) 027, arXiv:1207.5030 [hep-ph].
- [21] NNPDF Collaboration, R. Ball, et al., Parton distributions for the LHC Run II, *J. High Energy Phys.* 04 (2015) 040, arXiv:1410.8849 [hep-ph].
- [22] M.L. Mangano, F. Piccinini, A. Polosa, M. Moretti, R. Pittau, ALPGEN, a generator for hard multiparton processes in hadronic collisions, *J. High Energy Phys.* 07 (2003) 001, arXiv:hep-ph/0206293.
- [23] J. Alwall, et al., The automated computation of tree-level and next-to-leading order differential cross sections, and their matching to parton shower simulations, *J. High Energy Phys.* 07 (2014) 079, arXiv:1405.0301 [hep-ph].
- [24] T. Sjöstrand, S. Mrenna, P.Z. Skands, PYTHIA 6.4 physics and manual, *J. High Energy Phys.* 05 (2006) 026, arXiv:hep-ph/0603175.
- [25] P.Z. Skands, Tuning Monte Carlo generators: the Perugia tunes, *Phys. Rev. D* 82 (2010) 074018, arXiv:1005.3457 [hep-ph].
- [26] J. Pumplin, et al., New generation of parton distributions with uncertainties from global QCD analysis, *J. High Energy Phys.* 07 (2002) 012, arXiv:hep-ph/0201195.
- [27] ATLAS Collaboration, ATLAS Pythia 8 Tunes to 7 TeV Data, ATL-PHYS-PUB-2014-021, 2014–2014, <https://cds.cern.ch/record/1966419>.
- [28] NNPDF Collaboration, R. Ball, et al., Parton distributions with LHC data, *Nucl. Phys. B* 867 (2013) 244, arXiv:1207.1303 [hep-ph].
- [29] C. Anastasiou, L.J. Dixon, K. Melnikov, F. Petriello, High precision QCD at hadron colliders: electroweak gauge boson rapidity distributions at next-to-next-to leading order, *Phys. Rev. D* 69 (2004) 094008, arXiv:hep-ph/0312266.
- [30] R. Gavin, Y. Li, F. Petriello, S. Quackenbush, FEWZ 2.0: a code for hadronic Z production at next-to-next-to-leading order, *Comput. Phys. Commun.* 182 (2011) 2388, arXiv:1011.3540 [hep-ph].
- [31] Y. Li, F. Petriello, Combining QCD and electroweak corrections to dilepton production in the framework of the FEWZ simulation code, *Phys. Rev. D* 86 (2012) 094034, arXiv:1208.5967 [hep-ph].
- [32] M. Czakon, A. Mitov, Top++: a program for the calculation of the top-pair cross-section at hadron colliders, *Comput. Phys. Commun.* 185 (2014) 2930, arXiv:1112.5675 [hep-ph].
- [33] S. Agostinelli, et al., GEANT4 – a simulation toolkit, *Nucl. Instrum. Methods A* 506 (2003) 250.
- [34] ATLAS Collaboration, The ATLAS simulation infrastructure, *Eur. Phys. J. C* 70 (2010) 823, arXiv:1005.4568 [physics.ins-det].
- [35] ATLAS Collaboration, Summary of ATLAS Pythia 8 Tunes, ATL-PHYS-PUB-2012-003, 2012, <https://cds.cern.ch/record/1474107>.
- [36] A.D. Martin, W.J. Stirling, R.S. Thorne, G. Watt, Parton distributions for the LHC, *Eur. Phys. J. C* 63 (2009) 189, arXiv:0901.0002 [hep-ph].
- [37] ATLAS Collaboration, Electron Efficiency Measurements with the ATLAS Detector Using the 2015 LHC Proton–Proton Collision Data, ATLAS-CONF-2016-024, 2016, <https://cds.cern.ch/record/2157687>.
- [38] ATLAS Collaboration, Muon reconstruction performance of the ATLAS detector in proton–proton collision data at $\sqrt{s} = 13$ TeV, *Eur. Phys. J. C* 76 (2016) 292, arXiv:1603.05598 [hep-ex].
- [39] W. Lampl, et al., Calorimeter Clustering Algorithms: Description and Performance, ATL-LARG-PUB-2008-002, 2008, <https://cds.cern.ch/record/1099735>.
- [40] M. Cacciari, G.P. Salam, G. Soyez, The anti- k_t jet clustering algorithm, *J. High Energy Phys.* 04 (2008) 063, arXiv:0802.1189 [hep-ph].
- [41] M. Cacciari, G.P. Salam, G. Soyez, FastJet user manual, *Eur. Phys. J. C* 72 (2012) 1896, arXiv:1111.6097 [hep-ph].
- [42] ATLAS Collaboration, Jet energy scale measurements and their systematic uncertainties in proton–proton collisions at $\sqrt{s} = 13$ TeV with the ATLAS detector, arXiv:1703.09665 [hep-ex], 2017.
- [43] ATLAS Collaboration, Tagging and Suppression of Pileup Jets with the ATLAS Detector, ATLAS-CONF-2014-018, 2014, <https://cds.cern.ch/record/1700870>.
- [44] D.L. Rainwater, R. Szalapski, D. Zeppenfeld, Probing color singlet exchange in Z + two jet events at the CERN LHC, *Phys. Rev. D* 54 (1996) 6680, arXiv:hep-ph/9605444.
- [45] ATLAS Collaboration, Multi-Boson Simulation for 13 TeV ATLAS Analyses, ATL-PHYS-PUB-2016-002, 2016, <https://cds.cern.ch/record/2119986>.
- [46] M. Bahr, et al., Herwig++ physics and manual, *Eur. Phys. J. C* 58 (2008) 639, arXiv:0803.0883 [hep-ph].
- [47] ATLAS Collaboration, Luminosity determination in pp collisions at $\sqrt{s} = 8$ TeV using the ATLAS detector at the LHC, *Eur. Phys. J. C* 76 (2016) 653, arXiv:1608.03953 [hep-ex].
- [48] ATLAS Collaboration, Measurements of the production cross section of a Z boson in association with jets in pp collisions at $\sqrt{s} = 13$ TeV with the ATLAS detector, *Eur. Phys. J. C* 77 (2017) 361, arXiv:1702.05725 [hep-ex].
- [49] DØ Collaboration, V.M. Abazov, et al., Studies of W boson plus jets production in $p\bar{p}$ collisions at $\sqrt{s} = 1.96$ TeV, *Phys. Rev. D* 88 (2013) 092001, arXiv:1302.6508 [hep-ex].
- [50] CMS Collaboration, Measurements of differential cross sections for associated production of a W boson and jets in proton–proton collisions at $\sqrt{s} = 8$ TeV, *Phys. Rev. D* 95 (2017) 052002, arXiv:1610.04222 [hep-ex].
- [51] ATLAS Collaboration, Measurements of electroweak W_{jj} production and constraints on anomalous gauge couplings with the ATLAS detector, *Eur. Phys. J. C* 77 (2017) 474, arXiv:1703.04362 [hep-ex].
- [52] W. Verkerke, D. Kirkby, The RooFit toolkit for data modeling, arXiv:physics/0306116, 2003.
- [53] ATLAS Collaboration, ATLAS Computing Acknowledgements 2016–2017, 2016, ATL-GEN-PUB-2016-002, <http://cdsweb.cern.ch/record/2202407>.

The ATLAS Collaboration

M. Aaboud^{137d}, G. Aad⁸⁸, B. Abbott¹¹⁵, O. Abidinov^{12,*}, B. Abeloos¹¹⁹, S.H. Abidi¹⁶¹, O.S. AbouZeid¹³⁹, N.L. Abraham¹⁵¹, H. Abramowicz¹⁵⁵, H. Abreu¹⁵⁴, R. Abreu¹¹⁸, Y. Abulaiti^{148a,148b}, B.S. Acharya^{167a,167b,a}, S. Adachi¹⁵⁷, L. Adamczyk^{41a}, J. Adelman¹¹⁰, M. Adersberger¹⁰², T. Adye¹³³, A.A. Affolder¹³⁹, Y. Afik¹⁵⁴, T. Agatonovic-Jovin¹⁴, C. Agheorghiesei^{28c}, J.A. Aguilar-Saavedra^{128a,128f}, S.P. Ahlen²⁴, F. Ahmadov^{68,b}, G. Aielli^{135a,135b}, S. Akatsuka⁷¹, H. Akerstedt^{148a,148b}, T.P.A. Åkesson⁸⁴, E. Akilli⁵², A.V. Akimov⁹⁸, G.L. Alberghi^{22a,22b}, J. Albert¹⁷², P. Albicocco⁵⁰, M.J. Alconada Verzini⁷⁴, S.C. Alderweireldt¹⁰⁸, M. Aleksa³², I.N. Aleksandrov⁶⁸, C. Alexa^{28b}, G. Alexander¹⁵⁵, T. Alexopoulos¹⁰, M. Alhroob¹¹⁵, B. Ali¹³⁰, M. Aliev^{76a,76b}, G. Alimonti^{94a}, J. Alison³³, S.P. Alkire³⁸, B.M.M. Allbrooke¹⁵¹, B.W. Allen¹¹⁸, P.P. Allport¹⁹, A. Aloisio^{106a,106b}, A. Alonso³⁹, F. Alonso⁷⁴, C. Alpigiani¹⁴⁰, A.A. Alshehri⁵⁶, M.I. Alstady⁸⁸, B. Alvarez Gonzalez³², D. Álvarez Piqueras¹⁷⁰, M.G. Alvigi^{106a,106b}, B.T. Amadio¹⁶, Y. Amaral Coutinho^{26a}, C. Amelung²⁵, D. Amidei⁹², S.P. Amor Dos Santos^{128a,128c}, S. Amoroso³², G. Amundsen²⁵, C. Anastopoulos¹⁴¹, L.S. Ancu⁵², N. Andari¹⁹, T. Andeen¹¹, C.F. Anders^{60b}, J.K. Anders⁷⁷, K.J. Anderson³³, A. Andreazza^{94a,94b}, V. Andrei^{60a}, S. Angelidakis³⁷, I. Angelozzi¹⁰⁹, A. Angerami³⁸, A.V. Anisenkov^{111,c}, N. Anjos¹³, A. Annovi^{126a,126b}, C. Antel^{60a}, M. Antonelli⁵⁰, A. Antonov^{100,*}, D.J. Antrim¹⁶⁶, F. Anulli^{134a}, M. Aoki⁶⁹, L. Aperio Bella³², G. Arabidze⁹³, Y. Arai⁶⁹, J.P. Araque^{128a}, V. Araujo Ferraz^{26a}, A.T.H. Arce⁴⁸, R.E. Ardell⁸⁰, F.A. Arduh⁷⁴, J-F. Arguin⁹⁷, S. Argyropoulos⁶⁶, M. Arik^{20a}, A.J. Armbruster³², L.J. Armitage⁷⁹, O. Arnaez¹⁶¹,

H. Arnold⁵¹, M. Arratia³⁰, O. Arslan²³, A. Artamonov⁹⁹, G. Artoni¹²², S. Artz⁸⁶, S. Asai¹⁵⁷, N. Asbah⁴⁵, A. Ashkenazi¹⁵⁵, L. Asquith¹⁵¹, K. Assamagan²⁷, R. Astalos^{146a}, M. Atkinson¹⁶⁹, N.B. Atlay¹⁴³, K. Augsten¹³⁰, G. Avolio³², B. Axen¹⁶, M.K. Ayoub¹¹⁹, G. Azuelos^{97,d}, A.E. Baas^{60a}, M.J. Baca¹⁹, H. Bachacou¹³⁸, K. Bachas^{76a,76b}, M. Backes¹²², P. Bagnaia^{134a,134b}, M. Bahmani⁴², H. Bahrasemani¹⁴⁴, J.T. Baines¹³³, M. Bajic³⁹, O.K. Baker¹⁷⁹, E.M. Baldin^{111,c}, P. Balek¹⁷⁵, F. Balli¹³⁸, W.K. Balunas¹²⁴, E. Banas⁴², A. Bandyopadhyay²³, Sw. Banerjee^{176,e}, A.A.E. Bannoura¹⁷⁸, L. Barak¹⁵⁵, E.L. Barberio⁹¹, D. Barberis^{53a,53b}, M. Barbero⁸⁸, T. Barillari¹⁰³, M.-S. Barisits³², J.T. Barkeloo¹¹⁸, T. Barklow¹⁴⁵, N. Barlow³⁰, S.L. Barnes^{36c}, B.M. Barnett¹³³, R.M. Barnett¹⁶, Z. Barnovska-Blenessy^{36a}, A. Baroncelli^{136a}, G. Barone²⁵, A.J. Barr¹²², L. Barranco Navarro¹⁷⁰, F. Barreiro⁸⁵, J. Barreiro Guimarães da Costa^{35a}, R. Bartoldus¹⁴⁵, A.E. Barton⁷⁵, P. Bartos^{146a}, A. Basalaev¹²⁵, A. Bassalat^{119,f}, R.L. Bates⁵⁶, S.J. Batista¹⁶¹, J.R. Batley³⁰, M. Battaglia¹³⁹, M. Bause^{134a,134b}, F. Bauer¹³⁸, H.S. Bawa^{145,g}, J.B. Beacham¹¹³, M.D. Beattie⁷⁵, T. Beau⁸³, P.H. Beauchemin¹⁶⁵, P. Bechtel²³, H.P. Beck^{18,h}, H.C. Beck⁵⁷, K. Becker¹²², M. Becker⁸⁶, C. Becot¹¹², A.J. Beddall^{20d}, A. Beddall^{20b}, V.A. Bednyakov⁶⁸, M. Bedognetti¹⁰⁹, C.P. Bee¹⁵⁰, T.A. Beermann³², M. Begalli^{26a}, M. Begel²⁷, J.K. Behr⁴⁵, A.S. Bell⁸¹, G. Bella¹⁵⁵, L. Bellagamba^{22a}, A. Bellerive³¹, M. Bellomo¹⁵⁴, K. Belotskiy¹⁰⁰, O. Beltramello³², N.L. Belyaev¹⁰⁰, O. Benary^{155,*}, D. Benchekroun^{137a}, M. Bender¹⁰², K. Bendtz^{148a,148b}, N. Benekos¹⁰, Y. Benhammou¹⁵⁵, E. Benhar Nocchioli¹⁷⁹, J. Benitez⁶⁶, D.P. Benjamin⁴⁸, M. Benoit⁵², J.R. Bensinger²⁵, S. Bentvelsen¹⁰⁹, L. Beresford¹²², M. Beretta⁵⁰, D. Berge¹⁰⁹, E. Bergeas Kuutmann¹⁶⁸, N. Berger⁵, J. Beringer¹⁶, S. Berlendis⁵⁸, N.R. Bernard⁸⁹, G. Bernardi⁸³, C. Bernius¹⁴⁵, F.U. Bernlochner²³, T. Berry⁸⁰, P. Berta⁸⁶, C. Bertella^{35a}, G. Bertoli^{148a,148b}, F. Bertolucci^{126a,126b}, I.A. Bertram⁷⁵, C. Bertsche⁴⁵, D. Bertsche¹¹⁵, G.J. Besjes³⁹, O. Bessidskaia Bylund^{148a,148b}, M. Bessner⁴⁵, N. Besson¹³⁸, A. Bethani⁸⁷, S. Bethke¹⁰³, A.J. Bevan⁷⁹, J. Beyer¹⁰³, R.M. Bianchi¹²⁷, O. Biebel¹⁰², D. Biedermann¹⁷, R. Bielski⁸⁷, K. Bierwagen⁸⁶, N.V. Biesuz^{126a,126b}, M. Biglietti^{136a}, T.R.V. Billoud⁹⁷, H. Bilokon⁵⁰, M. Bindi⁵⁷, A. Bingul^{20b}, C. Bini^{134a,134b}, S. Biondi^{22a,22b}, T. Bisanz⁵⁷, C. Bittrich⁴⁷, D.M. Bjergaard⁴⁸, J.E. Black¹⁴⁵, K.M. Black²⁴, R.E. Blair⁶, T. Blazek^{146a}, I. Bloch⁴⁵, C. Blocker²⁵, A. Blue⁵⁶, W. Blum^{86,*}, U. Blumenschein⁷⁹, S. Blunier^{34a}, G.J. Bobbink¹⁰⁹, V.S. Bobrovnikov^{111,c}, S.S. Bocchetta⁸⁴, A. Bocci⁴⁸, C. Bock¹⁰², M. Boehler⁵¹, D. Boerner¹⁷⁸, D. Bogavac¹⁰², A.G. Bogdanchikov¹¹¹, C. Bohm^{148a}, V. Boisvert⁸⁰, P. Boka^{168,i}, T. Bold^{41a}, A.S. Boldyrev¹⁰¹, A.E. Bolz^{60b}, M. Bomben⁸³, M. Bona⁷⁹, M. Boonekamp¹³⁸, A. Borisov¹³², G. Borissov⁷⁵, J. Bortfeldt³², D. Bortoletto¹²², V. Bortolotto^{62a,62b,62c}, D. Boscherini^{22a}, M. Bosman¹³, J.D. Bossio Sola²⁹, J. Boudreau¹²⁷, J. Bouffard², E.V. Bouhova-Thacker⁷⁵, D. Boumediene³⁷, C. Bourdarios¹¹⁹, S.K. Boutle⁵⁶, A. Boveia¹¹³, J. Boyd³², I.R. Boyko⁶⁸, J. Bracinik¹⁹, A. Brandt⁸, G. Brandt⁵⁷, O. Brandt^{60a}, U. Bratzler¹⁵⁸, B. Brau⁸⁹, J.E. Brau¹¹⁸, W.D. Breaden Madden⁵⁶, K. Brendlinger⁴⁵, A.J. Brennan⁹¹, L. Brenner¹⁰⁹, R. Brenner¹⁶⁸, S. Bressler¹⁷⁵, D.L. Briglin¹⁹, T.M. Bristow⁴⁹, D. Britton⁵⁶, D. Britzger⁴⁵, F.M. Brochu³⁰, I. Brock²³, R. Brock⁹³, G. Brooijmans³⁸, T. Brooks⁸⁰, W.K. Brooks^{34b}, J. Brosamer¹⁶, E. Brost¹¹⁰, J.H. Broughton¹⁹, P.A. Bruckman de Renstrom⁴², D. Bruncko^{146b}, A. Bruni^{22a}, G. Bruni^{22a}, L.S. Bruni¹⁰⁹, B.H. Brunt³⁰, M. Bruschi^{22a}, N. Bruscino²³, P. Bryant³³, L. Bryngemark⁴⁵, T. Buane¹⁵, Q. Buat¹⁴⁴, P. Buchholz¹⁴³, A.G. Buckley⁵⁶, I.A. Budagov⁶⁸, F. Buehrer⁵¹, M.K. Bugge¹²¹, O. Bulekov¹⁰⁰, D. Bullock⁸, T.J. Burch¹¹⁰, S. Burdin⁷⁷, C.D. Burgard⁵¹, A.M. Burger⁵, B. Burghgrave¹¹⁰, K. Burka⁴², S. Burke¹³³, I. Burmeister⁴⁶, J.T.P. Burr¹²², E. Busato³⁷, D. Büscher⁵¹, V. Büscher⁸⁶, P. Bussey⁵⁶, J.M. Butler²⁴, C.M. Buttar⁵⁶, J.M. Butterworth⁸¹, P. Butti³², W. Buttinger²⁷, A. Buzatu¹⁵³, A.R. Buzykaev^{111,c}, S. Cabrera Urbán¹⁷⁰, D. Caforio¹³⁰, V.M. Cairo^{40a,40b}, O. Cakir^{4a}, N. Calace⁵², P. Calafiura¹⁶, A. Calandri⁸⁸, G. Calderini⁸³, P. Calfayan⁶⁴, G. Callea^{40a,40b}, L.P. Caloba^{26a}, S. Calvente Lopez⁸⁵, D. Calvet³⁷, S. Calvet³⁷, T.P. Calvet⁸⁸, R. Camacho Toro³³, S. Camarda³², P. Camarri^{135a,135b}, D. Cameron¹²¹, R. Caminal Armadans¹⁶⁹, C. Camincher⁵⁸, S. Campana³², M. Campanelli⁸¹, A. Camplani^{94a,94b}, A. Campoverde¹⁴³, V. Canale^{106a,106b}, M. Cano Bret^{36c}, J. Cantero¹¹⁶, T. Cao¹⁵⁵, M.D.M. Capeans Garrido³², I. Caprini^{28b}, M. Caprini^{28b}, M. Capua^{40a,40b}, R.M. Carbone³⁸, R. Cardarelli^{135a}, F. Cardillo⁵¹, I. Carli¹³¹, T. Carli³², G. Carlino^{106a}, B.T. Carlson¹²⁷, L. Carminati^{94a,94b}, R.M.D. Carney^{148a,148b}, S. Caron¹⁰⁸, E. Carquin^{34b}, S. Carrá^{94a,94b}, G.D. Carrillo-Montoya³², D. Casadei¹⁹, M.P. Casado^{13,j}, M. Casolino¹³, D.W. Casper¹⁶⁶, R. Castelijns¹⁰⁹, V. Castillo Gimenez¹⁷⁰, N.F. Castro^{128a,k}, A. Catinaccio³², J.R. Catmore¹²¹, A. Cattai³², J. Caudron²³, V. Cavaliere¹⁶⁹, E. Cavallaro¹³, D. Cavalli^{94a}, M. Cavalli-Sforza¹³, V. Cavasinni^{126a,126b}, E. Celebi^{20c}, F. Ceradini^{136a,136b}, L. Cerda Alberich¹⁷⁰, A.S. Cerqueira^{26b}, A. Cerri¹⁵¹, L. Cerrito^{135a,135b}, F. Cerutti¹⁶,

A. Cervelli ¹⁸, S.A. Cetin ^{20c}, A. Chafaq ^{137a}, D. Chakraborty ¹¹⁰, S.K. Chan ⁵⁹, W.S. Chan ¹⁰⁹, Y.L. Chan ^{62a}, P. Chang ¹⁶⁹, J.D. Chapman ³⁰, D.G. Charlton ¹⁹, C.C. Chau ³¹, C.A. Chavez Barajas ¹⁵¹, S. Che ¹¹³, S. Cheatham ^{167a,167c}, A. Chegwidan ⁹³, S. Chekanov ⁶, S.V. Chekulaev ^{163a}, G.A. Chelkov ^{68,l}, M.A. Chelstowska ³², C. Chen ⁶⁷, H. Chen ²⁷, J. Chen ^{36a}, S. Chen ^{35b}, S. Chen ¹⁵⁷, X. Chen ^{35c,m}, Y. Chen ⁷⁰, H.C. Cheng ⁹², H.J. Cheng ^{35a}, A. Cheplakov ⁶⁸, E. Cheremushkina ¹³², R. Cherkaoui El Moursli ^{137e}, E. Cheu ⁷, K. Cheung ⁶³, L. Chevalier ¹³⁸, V. Chiarella ⁵⁰, G. Chiarelli ^{126a,126b}, G. Chiodini ^{76a}, A.S. Chisholm ³², A. Chitan ^{28b}, Y.H. Chiu ¹⁷², M.V. Chizhov ⁶⁸, K. Choi ⁶⁴, A.R. Chomont ³⁷, S. Chouridou ¹⁵⁶, Y.S. Chow ^{62a}, V. Christodoulou ⁸¹, M.C. Chu ^{62a}, J. Chudoba ¹²⁹, A.J. Chuinard ⁹⁰, J.J. Chwastowski ⁴², L. Chytka ¹¹⁷, A.K. Ciftci ^{4a}, D. Cinca ⁴⁶, V. Cindro ⁷⁸, I.A. Cioara ²³, C. Ciocca ^{22a,22b}, A. Ciochio ¹⁶, F. Ciotto ^{106a,106b}, Z.H. Citron ¹⁷⁵, M. Citterio ^{94a}, M. Ciubancan ^{28b}, A. Clark ⁵², B.L. Clark ⁵⁹, M.R. Clark ³⁸, P.J. Clark ⁴⁹, R.N. Clarke ¹⁶, C. Clement ^{148a,148b}, Y. Coadou ⁸⁸, M. Cobal ^{167a,167c}, A. Coccaro ⁵², J. Cochran ⁶⁷, L. Colasurdo ¹⁰⁸, B. Cole ³⁸, A.P. Colijn ¹⁰⁹, J. Collot ⁵⁸, T. Colombo ¹⁶⁶, P. Conde Muino ^{128a,128b}, E. Coniavitis ⁵¹, S.H. Connell ^{147b}, I.A. Connolly ⁸⁷, S. Constantinescu ^{28b}, G. Conti ³², F. Conventi ^{106a,n}, M. Cooke ¹⁶, A.M. Cooper-Sarkar ¹²², F. Cormier ¹⁷¹, K.J.R. Cormier ¹⁶¹, M. Corradi ^{134a,134b}, F. Corriveau ^{90,o}, A. Cortes-Gonzalez ³², G. Cortiana ¹⁰³, G. Costa ^{94a}, M.J. Costa ¹⁷⁰, D. Costanzo ¹⁴¹, G. Cottin ³⁰, G. Cowan ⁸⁰, B.E. Cox ⁸⁷, K. Cranmer ¹¹², S.J. Crawley ⁵⁶, R.A. Creager ¹²⁴, G. Cree ³¹, S. Crépé-Renaudin ⁵⁸, F. Crescioli ⁸³, W.A. Cribbs ^{148a,148b}, M. Cristinziani ²³, V. Croft ¹⁰⁸, G. Crosetti ^{40a,40b}, A. Cueto ⁸⁵, T. Cuhadar Donszelmann ¹⁴¹, A.R. Cukierman ¹⁴⁵, J. Cummings ¹⁷⁹, M. Curatolo ⁵⁰, J. Cúth ⁸⁶, S. Czekierda ⁴², P. Czodrowski ³², G. D'amen ^{22a,22b}, S. D'Auria ⁵⁶, L. D'eraimo ⁸³, M. D'Onofrio ⁷⁷, M.J. Da Cunha Sargedas De Sousa ^{128a,128b}, C. Da Via ⁸⁷, W. Dabrowski ^{41a}, T. Dado ^{146a}, T. Dai ⁹², O. Dale ¹⁵, F. Dallaire ⁹⁷, C. Dallapiccola ⁸⁹, M. Dam ³⁹, J.R. Dandoy ¹²⁴, M.F. Daneri ²⁹, N.P. Dang ¹⁷⁶, A.C. Daniells ¹⁹, N.S. Dann ⁸⁷, M. Danninger ¹⁷¹, M. Dano Hoffmann ¹³⁸, V. Dao ¹⁵⁰, G. Darbo ^{53a}, S. Darmora ⁸, J. Dassoulas ³, A. Dattagupta ¹¹⁸, T. Daubney ⁴⁵, W. Davey ²³, C. David ⁴⁵, T. Davidek ¹³¹, D.R. Davis ⁴⁸, P. Davison ⁸¹, E. Dawe ⁹¹, I. Dawson ¹⁴¹, K. De ⁸, R. de Asmundis ^{106a}, A. De Benedetti ¹¹⁵, S. De Castro ^{22a,22b}, S. De Cecco ⁸³, N. De Groot ¹⁰⁸, P. de Jong ¹⁰⁹, H. De la Torre ⁹³, F. De Lorenzi ⁶⁷, A. De Maria ⁵⁷, D. De Pedis ^{134a}, A. De Salvo ^{134a}, U. De Sanctis ^{135a,135b}, A. De Santo ¹⁵¹, K. De Vasconcelos Corga ⁸⁸, J.B. De Vivie De Regie ¹¹⁹, R. Debbe ²⁷, C. Debenedetti ¹³⁹, D.V. Dedovich ⁶⁸, N. Dehghanian ³, I. Deigaard ¹⁰⁹, M. Del Gaudio ^{40a,40b}, J. Del Peso ⁸⁵, D. Delgove ¹¹⁹, F. Deliot ¹³⁸, C.M. Delitzsch ⁷, A. Dell'Acqua ³², L. Dell'Asta ²⁴, M. Dell'Orso ^{126a,126b}, M. Della Pietra ^{106a,106b}, D. della Volpe ⁵², M. Delmastro ⁵, C. Delporte ¹¹⁹, P.A. Delsart ⁵⁸, D.A. DeMarco ¹⁶¹, S. Demers ¹⁷⁹, M. Demichev ⁶⁸, A. Demilly ⁸³, S.P. Denisov ¹³², D. Denysiuk ¹³⁸, D. Derendarz ⁴², J.E. Derkaoui ^{137d}, F. Derue ⁸³, P. Dervan ⁷⁷, K. Desch ²³, C. Deterre ⁴⁵, K. Dette ¹⁶¹, M.R. Devesa ²⁹, P.O. Deviveiros ³², A. Dewhurst ¹³³, S. Dhaliwal ²⁵, F.A. Di Bello ⁵², A. Di Ciaccio ^{135a,135b}, L. Di Ciaccio ⁵, W.K. Di Clemente ¹²⁴, C. Di Donato ^{106a,106b}, A. Di Girolamo ³², B. Di Girolamo ³², B. Di Micco ^{136a,136b}, R. Di Nardo ³², K.F. Di Petrillo ⁵⁹, A. Di Simone ⁵¹, R. Di Sipio ¹⁶¹, D. Di Valentino ³¹, C. Diaconu ⁸⁸, M. Diamond ¹⁶¹, F.A. Dias ³⁹, M.A. Diaz ^{34a}, E.B. Diehl ⁹², J. Dietrich ¹⁷, S. Díez Cornell ⁴⁵, A. Dimitrievska ¹⁴, J. Dingfelder ²³, P. Dita ^{28b}, S. Dita ^{28b}, F. Dittus ³², F. Djama ⁸⁸, T. Djobava ^{54b}, J.I. Djuvsland ^{60a}, M.A.B. do Vale ^{26c}, D. Dobos ³², M. Dobre ^{28b}, C. Doglioni ⁸⁴, J. Dolejsi ¹³¹, Z. Dolezal ¹³¹, M. Donadelli ^{26d}, S. Donati ^{126a,126b}, P. Dondero ^{123a,123b}, J. Donini ³⁷, J. Dopke ¹³³, A. Doria ^{106a}, M.T. Dova ⁷⁴, A.T. Doyle ⁵⁶, E. Drechsler ⁵⁷, M. Dris ¹⁰, Y. Du ^{36b}, J. Duarte-Campderros ¹⁵⁵, A. Dubreuil ⁵², E. Duchovni ¹⁷⁵, G. Duckeck ¹⁰², A. Ducourthial ⁸³, O.A. Ducu ^{97,p}, D. Duda ¹⁰⁹, A. Dudarev ³², A.Ch. Dudder ⁸⁶, E.M. Duffield ¹⁶, L. Duflo ¹¹⁹, M. Dührssen ³², M. Dumancic ¹⁷⁵, A.E. Dumitriu ^{28b}, A.K. Duncan ⁵⁶, M. Dunford ^{60a}, H. Duran Yildiz ^{4a}, M. Düren ⁵⁵, A. Durglishvili ^{54b}, D. Duschinger ⁴⁷, B. Dutta ⁴⁵, D. Duvnjak ¹, M. Dyndal ⁴⁵, B.S. Dziedzic ⁴², C. Eckardt ⁴⁵, K.M. Ecker ¹⁰³, R.C. Edgar ⁹², T. Eifert ³², G. Eigen ¹⁵, K. Einsweiler ¹⁶, T. Ekelof ¹⁶⁸, M. El Kacimi ^{137c}, R. El Kosseifi ⁸⁸, V. Ellajosyula ⁸⁸, M. Ellert ¹⁶⁸, S. Elles ⁵, F. Ellinghaus ¹⁷⁸, A.A. Elliot ¹⁷², N. Ellis ³², J. Elmsheuser ²⁷, M. Elsing ³², D. Emeliyanov ¹³³, Y. Enari ¹⁵⁷, O.C. Endner ⁸⁶, J.S. Ennis ¹⁷³, J. Erdmann ⁴⁶, A. Ereditato ¹⁸, M. Ernst ²⁷, S. Errede ¹⁶⁹, M. Escalier ¹¹⁹, C. Escobar ¹⁷⁰, B. Esposito ⁵⁰, O. Estrada Pastor ¹⁷⁰, A.I. Etiennevre ¹³⁸, E. Etzion ¹⁵⁵, H. Evans ⁶⁴, A. Ezhilov ¹²⁵, M. Ezzi ^{137e}, F. Fabbri ^{22a,22b}, L. Fabbri ^{22a,22b}, V. Fabiani ¹⁰⁸, G. Facini ⁸¹, R.M. Fakhruddinov ¹³², S. Falciano ^{134a}, R.J. Falla ⁸¹, J. Faltova ³², Y. Fang ^{35a}, M. Fanti ^{94a,94b}, A. Farbin ⁸, A. Farilla ^{136a}, C. Farina ¹²⁷, E.M. Farina ^{123a,123b}, T. Farooque ⁹³, S. Farrell ¹⁶, S.M. Farrington ¹⁷³, P. Farthouat ³², F. Fassi ^{137e}, P. Fassnacht ³², D. Fassouliotis ⁹, M. Fauci Giannelli ⁴⁹,

A. Favareto^{53a,53b}, W.J. Fawcett¹²², L. Fayard¹¹⁹, O.L. Fedin^{125,q}, W. Fedorko¹⁷¹, S. Feigl¹²¹, L. Feligioni⁸⁸, C. Feng^{36b}, E.J. Feng³², H. Feng⁹², M.J. Fenton⁵⁶, A.B. Fenyuk¹³², L. Feremenga⁸, P. Fernandez Martinez¹⁷⁰, S. Fernandez Perez¹³, J. Ferrando⁴⁵, A. Ferrari¹⁶⁸, P. Ferrari¹⁰⁹, R. Ferrari^{123a}, D.E. Ferreira de Lima^{60b}, A. Ferrer¹⁷⁰, D. Ferrere⁵², C. Ferretti⁹², F. Fiedler⁸⁶, A. Filipčič⁷⁸, M. Filipuzzi⁴⁵, F. Filthaut¹⁰⁸, M. Fincke-Keeler¹⁷², K.D. Finelli¹⁵², M.C.N. Fiolhais^{128a,128c,r}, L. Fiorini¹⁷⁰, A. Fischer², C. Fischer¹³, J. Fischer¹⁷⁸, W.C. Fisher⁹³, N. Flaschel⁴⁵, I. Fleck¹⁴³, P. Fleischmann⁹², R.R.M. Fletcher¹²⁴, T. Flick¹⁷⁸, B.M. Flierl¹⁰², L.R. Flores Castillo^{62a}, M.J. Flowerdew¹⁰³, G.T. Forcolin⁸⁷, A. Formica¹³⁸, F.A. Förster¹³, A. Forti⁸⁷, A.G. Foster¹⁹, D. Fournier¹¹⁹, H. Fox⁷⁵, S. Fracchia¹⁴¹, P. Francavilla⁸³, M. Franchini^{22a,22b}, S. Franchino^{60a}, D. Francis³², L. Franconi¹²¹, M. Franklin⁵⁹, M. Frate¹⁶⁶, M. Fraternali^{123a,123b}, D. Freeborn⁸¹, S.M. Fressard-Batraneanu³², B. Freund⁹⁷, D. Froidevaux³², J.A. Frost¹²², C. Fukunaga¹⁵⁸, T. Fusayasu¹⁰⁴, J. Fuster¹⁷⁰, C. Gabaldon⁵⁸, O. Gabizon¹⁵⁴, A. Gabrielli^{22a,22b}, A. Gabrielli¹⁶, G.P. Gach^{41a}, S. Gadatsch³², S. Gadomski⁸⁰, G. Gagliardi^{53a,53b}, L.G. Gagnon⁹⁷, C. Galea¹⁰⁸, B. Galhardo^{128a,128c}, E.J. Gallas¹²², B.J. Gallop¹³³, P. Gallus¹³⁰, G. Galster³⁹, K.K. Gan¹¹³, S. Ganguly³⁷, Y. Gao⁷⁷, Y.S. Gao^{145,g}, F.M. Garay Walls^{34a}, C. García¹⁷⁰, J.E. García Navarro¹⁷⁰, J.A. García Pascual^{35a}, M. Garcia-Sciveres¹⁶, R.W. Gardner³³, N. Garelli¹⁴⁵, V. Garonne¹²¹, A. Gascon Bravo⁴⁵, K. Gasnikova⁴⁵, C. Gatti⁵⁰, A. Gaudiello^{53a,53b}, G. Gaudio^{123a}, I.L. Gavrilenko⁹⁸, C. Gay¹⁷¹, G. Gaycken²³, E.N. Gazis¹⁰, C.N.P. Gee¹³³, J. Geisen⁵⁷, M. Geisen⁸⁶, M.P. Geisler^{60a}, K. Gellerstedt^{148a,148b}, C. Gemme^{53a}, M.H. Genest⁵⁸, C. Geng⁹², S. Gentile^{134a,134b}, C. Gentsos¹⁵⁶, S. George⁸⁰, D. Gerbaudo¹³, A. Gershon¹⁵⁵, G. Geßner⁴⁶, S. Ghasemi¹⁴³, M. Ghneimat²³, B. Giacobbe^{22a}, S. Giagu^{134a,134b}, N. Giangiacomi^{22a,22b}, P. Giannetti^{126a,126b}, S.M. Gibson⁸⁰, M. Gignac¹⁷¹, M. Gilchriese¹⁶, D. Gillberg³¹, G. Gilles¹⁷⁸, D.M. Gingrich^{3,d}, M.P. Giordani^{167a,167c}, F.M. Giorgi^{22a}, P.F. Giraud¹³⁸, P. Giromini⁵⁹, G. Giugliarelli^{167a,167c}, D. Giugni^{94a}, F. Giuli¹²², C. Giuliani¹⁰³, M. Giulini^{60b}, B.K. Gjelsten¹²¹, S. Gkaitatzis¹⁵⁶, I. Gkialas^{9,s}, E.L. Gkougkousis¹³, P. Gkoutoumis¹⁰, L.K. Gladilin¹⁰¹, C. Glasman⁸⁵, J. Glatzer¹³, P.C.F. Glaysher⁴⁵, A. Glazov⁴⁵, M. Goblirsch-Kolb²⁵, J. Godlewski⁴², S. Goldfarb⁹¹, T. Golling⁵², D. Golubkov¹³², A. Gomes^{128a,128b,128d}, R. Gonçalves^{128a}, R. Goncalves Gama^{26a}, J. Goncalves Pinto Firmino Da Costa¹³⁸, G. Gonella⁵¹, L. Gonella¹⁹, A. Gongadze⁶⁸, S. González de la Hoz¹⁷⁰, S. Gonzalez-Sevilla⁵², L. Goossens³², P.A. Gorbounov⁹⁹, H.A. Gordon²⁷, I. Gorelov¹⁰⁷, B. Gorini³², E. Gorini^{76a,76b}, A. Gorišek⁷⁸, A.T. Goshaw⁴⁸, C. Gössling⁴⁶, M.I. Gostkin⁶⁸, C.A. Gottardo²³, C.R. Goudet¹¹⁹, D. Goujdami^{137c}, A.G. Goussiou¹⁴⁰, N. Govender^{147b,t}, E. Gozani¹⁵⁴, L. Graber⁵⁷, I. Grabowska-Bold^{41a}, P.O.J. Gradin¹⁶⁸, J. Gramling¹⁶⁶, E. Gramstad¹²¹, S. Grancagnolo¹⁷, V. Gratchev¹²⁵, P.M. Gravila^{28f}, C. Gray⁵⁶, H.M. Gray¹⁶, Z.D. Greenwood^{82,u}, C. Grefe²³, K. Gregersen⁸¹, I.M. Gregor⁴⁵, P. Grenier¹⁴⁵, K. Grevtsov⁵, J. Griffiths⁸, A.A. Grillo¹³⁹, K. Grimm⁷⁵, S. Grinstein^{13,v}, Ph. Gris³⁷, J.-F. Grivaz¹¹⁹, S. Groh⁸⁶, E. Gross¹⁷⁵, J. Grosse-Knetter⁵⁷, G.C. Grossi⁸², Z.J. Grout⁸¹, A. Grummer¹⁰⁷, L. Guan⁹², W. Guan¹⁷⁶, J. Guenther⁶⁵, F. Guescini^{163a}, D. Guest¹⁶⁶, O. Gueta¹⁵⁵, B. Gui¹¹³, E. Guido^{53a,53b}, T. Guillemin⁵, S. Guindon³², U. Gul⁵⁶, C. Gumpert³², J. Guo^{36c}, W. Guo⁹², Y. Guo^{36a}, R. Gupta⁴³, S. Gupta¹²², G. Gustavino¹¹⁵, B.J. Gutelman¹⁵⁴, P. Gutierrez¹¹⁵, N.G. Gutierrez Ortiz⁸¹, C. Gutsche⁸¹, C. Guyot¹³⁸, M.P. Guzik^{41a}, C. Gwenlan¹²², C.B. Gwilliam⁷⁷, A. Haas¹¹², C. Haber¹⁶, H.K. Hadavand⁸, N. Haddad^{137e}, A. Hadeef⁸⁸, S. Hageböck²³, M. Hagihara¹⁶⁴, H. Hakobyan^{180,*}, M. Haleem⁴⁵, J. Haley¹¹⁶, G. Halladjian⁹³, G.D. Hallewell⁸⁸, K. Hamacher¹⁷⁸, P. Hamal¹¹⁷, K. Hamano¹⁷², A. Hamilton^{147a}, G.N. Hamity¹⁴¹, P.G. Hamnett⁴⁵, L. Han^{36a}, S. Han^{35a}, K. Hanagaki^{69,w}, K. Hanawa¹⁵⁷, M. Hance¹³⁹, B. Haney¹²⁴, P. Hanke^{60a}, J.B. Hansen³⁹, J.D. Hansen³⁹, M.C. Hansen²³, P.H. Hansen³⁹, K. Hara¹⁶⁴, A.S. Hard¹⁷⁶, T. Harenberg¹⁷⁸, F. Hariri¹¹⁹, S. Harkusha⁹⁵, R.D. Harrington⁴⁹, P.F. Harrison¹⁷³, N.M. Hartmann¹⁰², Y. Hasegawa¹⁴², A. Hasib⁴⁹, S. Hassani¹³⁸, S. Haug¹⁸, R. Hauser⁹³, L. Hauswald⁴⁷, L.B. Havener³⁸, M. Havranek¹³⁰, C.M. Hawkes¹⁹, R.J. Hawking³², D. Hayakawa¹⁵⁹, D. Hayden⁹³, C.P. Hays¹²², J.M. Hays⁷⁹, H.S. Hayward⁷⁷, S.J. Haywood¹³³, S.J. Head¹⁹, T. Heck⁸⁶, V. Hedberg⁸⁴, L. Heelan⁸, S. Heer²³, K.K. Heidegger⁵¹, S. Heim⁴⁵, T. Heim¹⁶, B. Heinemann^{45,x}, J.J. Heinrich¹⁰², L. Heinrich¹¹², C. Heinz⁵⁵, J. Hejbal¹²⁹, L. Helary³², A. Held¹⁷¹, S. Hellman^{148a,148b}, C. Helsens³², R.C.W. Henderson⁷⁵, Y. Heng¹⁷⁶, S. Henkelmann¹⁷¹, A.M. Henriques Correia³², S. Henrot-Versille¹¹⁹, G.H. Herbert¹⁷, H. Herde²⁵, V. Herget¹⁷⁷, Y. Hernández Jiménez^{147c}, H. Herr⁸⁶, G. Herten⁵¹, R. Hertenberger¹⁰², L. Hervas³², T.C. Herwig¹²⁴, G.G. Hesketh⁸¹, N.P. Hessey^{163a}, J.W. Hetherly⁴³, S. Higashino⁶⁹, E. Higón-Rodriguez¹⁷⁰, K. Hildebrand³³, E. Hill¹⁷², J.C. Hill³⁰, K.H. Hiller⁴⁵, S.J. Hillier¹⁹,

M. Hils⁴⁷, I. Hinchliffe¹⁶, M. Hirose⁵¹, D. Hirschbuehl¹⁷⁸, B. Hiti⁷⁸, O. Hladik¹²⁹, X. Hoad⁴⁹, J. Hobbs¹⁵⁰, N. Hod^{163a}, M.C. Hodgkinson¹⁴¹, P. Hodgson¹⁴¹, A. Hoecker³², M.R. Hoferkamp¹⁰⁷, F. Hoenig¹⁰², D. Hohn²³, T.R. Holmes³³, M. Homann⁴⁶, S. Honda¹⁶⁴, T. Honda⁶⁹, T.M. Hong¹²⁷, B.H. Hooberman¹⁶⁹, W.H. Hopkins¹¹⁸, Y. Horii¹⁰⁵, A.J. Horton¹⁴⁴, J.-Y. Hostachy⁵⁸, S. Hou¹⁵³, A. Hoummada^{137a}, J. Howarth⁸⁷, J. Hoya⁷⁴, M. Hrabovsky¹¹⁷, J. Hrdinka³², I. Hristova¹⁷, J. Hrivnac¹¹⁹, T. Hryn'ova⁵, A. Hrynevich⁹⁶, P.J. Hsu⁶³, S.-C. Hsu¹⁴⁰, Q. Hu^{36a}, S. Hu^{36c}, Y. Huang^{35a}, Z. Hubacek¹³⁰, F. Hubaut⁸⁸, F. Huegging²³, T.B. Huffman¹²², E.W. Hughes³⁸, G. Hughes⁷⁵, M. Huhtinen³², P. Huo¹⁵⁰, N. Huseynov^{68,b}, J. Huston⁹³, J. Huth⁵⁹, G. Iacobucci⁵², G. Iakovidis²⁷, I. Ibragimov¹⁴³, L. Iconomidou-Fayard¹¹⁹, Z. Idrissi^{137e}, P. Iengo³², O. Igonkina^{109,y}, T. Iizawa¹⁷⁴, Y. Ikegami⁶⁹, M. Ikeno⁶⁹, Y. Ilchenko^{11,z}, D. Iliadis¹⁵⁶, N. Ilic¹⁴⁵, G. Introzzi^{123a,123b}, P. Ioannou^{9,*}, M. Iodice^{136a}, K. Iordanidou³⁸, V. Ippolito⁵⁹, M.F. Isacson¹⁶⁸, N. Ishijima¹²⁰, M. Ishino¹⁵⁷, M. Ishitsuka¹⁵⁹, C. Issever¹²², S. Istin^{20a}, F. Ito¹⁶⁴, J.M. Iturbe Ponce^{62a}, R. Iuppa^{162a,162b}, H. Iwasaki⁶⁹, J.M. Izen⁴⁴, V. Izzo^{106a}, S. Jabbar³, P. Jackson¹, R.M. Jacobs²³, V. Jain², K.B. Jakobi⁸⁶, K. Jakobs⁵¹, S. Jakobsen⁶⁵, T. Jakoubek¹²⁹, D.O. Jamin¹¹⁶, D.K. Jana⁸², R. Jansky⁵², J. Janssen²³, M. Janus⁵⁷, P.A. Janus^{41a}, G. Jarlskog⁸⁴, N. Javadov^{68,b}, T. Javůrek⁵¹, M. Javurkova⁵¹, F. Jeanneau¹³⁸, L. Jeanty¹⁶, J. Jejelava^{54a,aa}, A. Jelinskas¹⁷³, P. Jenni^{51,ab}, C. Jeske¹⁷³, S. Jézéquel⁵, H. Ji¹⁷⁶, J. Jia¹⁵⁰, H. Jiang⁶⁷, Y. Jiang^{36a}, Z. Jiang¹⁴⁵, S. Jiggins⁸¹, J. Jimenez Pena¹⁷⁰, S. Jin^{35a}, A. Jinaru^{28b}, O. Jinnouchi¹⁵⁹, H. Jivan^{147c}, P. Johansson¹⁴¹, K.A. Johns⁷, C.A. Johnson⁶⁴, W.J. Johnson¹⁴⁰, K. Jon-And^{148a,148b}, R.W.L. Jones⁷⁵, S.D. Jones¹⁵¹, S. Jones⁷, T.J. Jones⁷⁷, J. Jongmanns^{60a}, P.M. Jorge^{128a,128b}, J. Jovicevic^{163a}, X. Ju¹⁷⁶, A. Juste Rozas^{13,v}, M.K. Köhler¹⁷⁵, A. Kaczmarska⁴², M. Kado¹¹⁹, H. Kagan¹¹³, M. Kagan¹⁴⁵, S.J. Kahn⁸⁸, T. Kaji¹⁷⁴, E. Kajomovitz⁴⁸, C.W. Kalderon⁸⁴, A. Kaluza⁸⁶, S. Kama⁴³, A. Kamenshchikov¹³², N. Kanaya¹⁵⁷, L. Kanjir⁷⁸, V.A. Kantserov¹⁰⁰, J. Kanzaki⁶⁹, B. Kaplan¹¹², L.S. Kaplan¹⁷⁶, D. Kar^{147c}, K. Karakostas¹⁰, N. Karastathis¹⁰, M.J. Kareem⁵⁷, E. Karentzos¹⁰, S.N. Karpov⁶⁸, Z.M. Karpova⁶⁸, K. Karthik¹¹², V. Kartvelishvili⁷⁵, A.N. Karyukhin¹³², K. Kasahara¹⁶⁴, L. Kashif¹⁷⁶, R.D. Kass¹¹³, A. Kastanas¹⁴⁹, Y. Kataoka¹⁵⁷, C. Kato¹⁵⁷, A. Katre⁵², J. Katzy⁴⁵, K. Kawade⁷⁰, K. Kawagoe⁷³, T. Kawamoto¹⁵⁷, G. Kawamura⁵⁷, E.F. Kay⁷⁷, V.F. Kazanin^{111,c}, R. Keeler¹⁷², R. Kehoe⁴³, J.S. Keller³¹, E. Kellermann⁸⁴, J.J. Kempster⁸⁰, J. Kendrick¹⁹, H. Keoshkerian¹⁶¹, O. Kepka¹²⁹, B.P. Kerševan⁷⁸, S. Kersten¹⁷⁸, R.A. Keyes⁹⁰, M. Khader¹⁶⁹, F. Khalil-zada¹², A. Khanov¹¹⁶, A.G. Kharlamov^{111,c}, T. Kharlamova^{111,c}, A. Khodinov¹⁶⁰, T.J. Khoo⁵², V. Khovanskiy^{99,*}, E. Khramov⁶⁸, J. Khubua^{54b,ac}, S. Kido⁷⁰, C.R. Kilby⁸⁰, H.Y. Kim⁸, S.H. Kim¹⁶⁴, Y.K. Kim³³, N. Kimura¹⁵⁶, O.M. Kind¹⁷, B.T. King⁷⁷, D. Kirchmeier⁴⁷, J. Kirk¹³³, A.E. Kiryunin¹⁰³, T. Kishimoto¹⁵⁷, D. Kisielewska^{41a}, V. Kitali⁴⁵, O. Kivernyk⁵, E. Kladiva^{146b}, T. Klapdor-Kleingrothaus⁵¹, M.H. Klein³⁸, M. Klein⁷⁷, U. Klein⁷⁷, K. Kleinknecht⁸⁶, P. Klimek¹¹⁰, A. Klimentov²⁷, R. Klingenberg⁴⁶, T. Klingl²³, T. Klioutchnikova³², E.-E. Kluge^{60a}, P. Kluit¹⁰⁹, S. Kluth¹⁰³, E. Kneringer⁶⁵, E.B.F.G. Knoop⁸⁸, A. Knue¹⁰³, A. Kobayashi¹⁵⁷, D. Kobayashi¹⁵⁹, T. Kobayashi¹⁵⁷, M. Kobel⁴⁷, M. Kocian¹⁴⁵, P. Kodys¹³¹, T. Koffas³¹, E. Koffeman¹⁰⁹, N.M. Köhler¹⁰³, T. Koi¹⁴⁵, M. Kolb^{60b}, I. Koletsou⁵, A.A. Komar^{98,*}, T. Kondo⁶⁹, N. Kondrashova^{36c}, K. Köneke⁵¹, A.C. König¹⁰⁸, T. Kono^{69,ad}, R. Konoplich^{112,ae}, N. Konstantinidis⁸¹, R. Kopeliansky⁶⁴, S. Koperny^{41a}, A.K. Kopp⁵¹, K. Korcyl⁴², K. Kordas¹⁵⁶, A. Korn⁸¹, A.A. Korol^{111,c}, I. Korolkov¹³, E.V. Korolkova¹⁴¹, O. Kortner¹⁰³, S. Kortner¹⁰³, T. Kosek¹³¹, V.V. Kostyukhin²³, A. Kotwal⁴⁸, A. Koulouris¹⁰, A. Kourkouveli-Charalampidi^{123a,123b}, C. Kourkouvelis⁹, E. Kourlitis¹⁴¹, V. Kouskoura²⁷, A.B. Kowalewska⁴², R. Kowalewski¹⁷², T.Z. Kowalski^{41a}, C. Kozakai¹⁵⁷, W. Kozanecki¹³⁸, A.S. Kozhin¹³², V.A. Kramarenko¹⁰¹, G. Kramberger⁷⁸, D. Krasnopevtsev¹⁰⁰, M.W. Krasny⁸³, A. Krasznahorkay³², D. Krauss¹⁰³, J.A. Kremer^{41a}, J. Kretzschmar⁷⁷, K. Kreutzfeldt⁵⁵, P. Krieger¹⁶¹, K. Krizka¹⁶, K. Kroeninger⁴⁶, H. Kroha¹⁰³, J. Kroll¹²⁹, J. Kroll¹²⁴, J. Kroseberg²³, J. Krstic¹⁴, U. Kruchonak⁶⁸, H. Krüger²³, N. Krumnack⁶⁷, M.C. Kruse⁴⁸, T. Kubota⁹¹, H. Kucuk⁸¹, S. Kuday^{4b}, J.T. Kuechler¹⁷⁸, S. Kuehn³², A. Kugel^{60a}, F. Kuger¹⁷⁷, T. Kuhl⁴⁵, V. Kukhtin⁶⁸, R. Kukla⁸⁸, Y. Kulchitsky⁹⁵, S. Kuleshov^{34b}, Y.P. Kulinich¹⁶⁹, M. Kuna^{134a,134b}, T. Kunigo⁷¹, A. Kupco¹²⁹, T. Kupfer⁴⁶, O. Kuprash¹⁵⁵, H. Kurashige⁷⁰, L.L. Kurchaninov^{163a}, Y.A. Kurochkin⁹⁵, M.G. Kurth^{35a}, V. Kus¹²⁹, E.S. Kuwertz¹⁷², M. Kuze¹⁵⁹, J. Kvita¹¹⁷, T. Kwan¹⁷², D. Kyriazopoulos¹⁴¹, A. La Rosa¹⁰³, J.L. La Rosa Navarro^{26d}, L. La Rotonda^{40a,40b}, F. La Ruffa^{40a,40b}, C. Lacasta¹⁷⁰, F. Lacava^{134a,134b}, J. Lacey⁴⁵, D.P.J. Lack⁸⁷, H. Lacker¹⁷, D. Lacour⁸³, E. Ladygin⁶⁸, R. Lafaye⁵, B. Laforge⁸³, T. Lagouri¹⁷⁹, S. Lai⁵⁷, S. Lammers⁶⁴, W. Lampl⁷, E. Lançon²⁷, U. Landgraf⁵¹, M.P.J. Landon⁷⁹, M.C. Lanfermann⁵², V.S. Lang⁴⁵, J.C. Lange¹³,

R.J. Langenberg³², A.J. Lankford¹⁶⁶, F. Lanni²⁷, K. Lantzsch²³, A. Lanza^{123a}, A. Lapertosa^{53a,53b}, S. Laplace⁸³, J.F. Laporte¹³⁸, T. Lari^{94a}, F. Lasagni Manghi^{22a,22b}, M. Lassnig³², T.S. Lau^{62a}, P. Laurelli⁵⁰, W. Lavrijsen¹⁶, A.T. Law¹³⁹, P. Laycock⁷⁷, T. Lazovich⁵⁹, M. Lazzaroni^{94a,94b}, B. Le⁹¹, O. Le Dortz⁸³, E. Le Guirriec⁸⁸, E.P. Le Quilleuc¹³⁸, M. LeBlanc¹⁷², T. LeCompte⁶, F. Ledroit-Guillon⁵⁸, C.A. Lee²⁷, G.R. Lee^{133,af}, S.C. Lee¹⁵³, L. Lee⁵⁹, B. Lefebvre⁹⁰, G. Lefebvre⁸³, M. Lefebvre¹⁷², F. Legger¹⁰², C. Leggett¹⁶, G. Lehmann Miotto³², X. Lei⁷, W.A. Leight⁴⁵, M.A.L. Leite^{26d}, R. Leitner¹³¹, D. Lellouch¹⁷⁵, B. Lemmer⁵⁷, K.J.C. Leney⁸¹, T. Lenz²³, B. Lenzi³², R. Leone⁷, S. Leone^{126a,126b}, C. Leonidopoulos⁴⁹, G. Lerner¹⁵¹, C. Leroy⁹⁷, A.A.J. Lesage¹³⁸, C.G. Lester³⁰, M. Levchenko¹²⁵, J. Levêque⁵, D. Levin⁹², L.J. Levinson¹⁷⁵, M. Levy¹⁹, D. Lewis⁷⁹, B. Li^{36a,ag}, Changqiao Li^{36a}, H. Li¹⁵⁰, L. Li^{36c}, Q. Li^{35a}, Q. Li^{36a}, S. Li⁴⁸, X. Li^{36c}, Y. Li¹⁴³, Z. Liang^{35a}, B. Liberti^{135a}, A. Liblong¹⁶¹, K. Lie^{62c}, J. Liebal²³, W. Liebig¹⁵, A. Limosani¹⁵², S.C. Lin¹⁸², T.H. Lin⁸⁶, R.A. Linck⁶⁴, B.E. Lindquist¹⁵⁰, A.E. Lioni⁵², E. Lipeles¹²⁴, A. Lipniacka¹⁵, M. Lisovsky^{60b}, T.M. Liss^{169,ah}, A. Lister¹⁷¹, A.M. Litke¹³⁹, B. Liu⁶⁷, H. Liu⁹², H. Liu²⁷, J.K.K. Liu¹²², J. Liu^{36b}, J.B. Liu^{36a}, K. Liu⁸⁸, L. Liu¹⁶⁹, M. Liu^{36a}, Y.L. Liu^{36a}, Y. Liu^{36a}, M. Livan^{123a,123b}, A. Lleres⁵⁸, J. Llorente Merino^{35a}, S.L. Lloyd⁷⁹, C.Y. Lo^{62b}, F. Lo Sterzo¹⁵³, E.M. Lobodzinska⁴⁵, P. Loch⁷, F.K. Loebinger⁸⁷, A. Loesle⁵¹, K.M. Loew²⁵, A. Loginov^{179,*}, T. Lohse¹⁷, K. Lohwasser¹⁴¹, M. Lokajicek¹²⁹, B.A. Long²⁴, J.D. Long¹⁶⁹, R.E. Long⁷⁵, L. Longo^{76a,76b}, K.A. Looper¹¹³, J.A. Lopez^{34b}, D. Lopez Mateos⁵⁹, I. Lopez Paz¹³, A. Lopez Solis⁸³, J. Lorenz¹⁰², N. Lorenzo Martinez⁵, M. Losada²¹, P.J. Lösel¹⁰², X. Lou^{35a}, A. Lounis¹¹⁹, J. Love⁶, P.A. Love⁷⁵, H. Lu^{62a}, N. Lu⁹², Y.J. Lu⁶³, H.J. Lubatti¹⁴⁰, C. Luci^{134a,134b}, A. Lucotte⁵⁸, C. Luedtke⁵¹, F. Luehring⁶⁴, W. Lukas⁶⁵, L. Luminari^{134a}, O. Lundberg^{148a,148b}, B. Lund-Jensen¹⁴⁹, M.S. Lutz⁸⁹, P.M. Luzi⁸³, D. Lynn²⁷, R. Lysak¹²⁹, E. Lytken⁸⁴, F. Lyu^{35a}, V. Lyubushkin⁶⁸, H. Ma²⁷, L.L. Ma^{36b}, Y. Ma^{36b}, G. Maccarrone⁵⁰, A. Macchiolo¹⁰³, C.M. Macdonald¹⁴¹, B. Maček⁷⁸, J. Machado Miguens^{124,128b}, D. Madaffari¹⁷⁰, R. Madar³⁷, W.F. Mader⁴⁷, A. Madsen⁴⁵, J. Maeda⁷⁰, S. Maeland¹⁵, T. Maeno²⁷, A.S. Maevskiy¹⁰¹, V. Magerl⁵¹, J. Mahlstedt¹⁰⁹, C. Maiani¹¹⁹, C. Maidantchik^{26a}, A.A. Maier¹⁰³, T. Maier¹⁰², A. Maio^{128a,128b,128d}, O. Majersky^{146a}, S. Majewski¹¹⁸, Y. Makida⁶⁹, N. Makovec¹¹⁹, B. Malaescu⁸³, Pa. Malecki⁴², V.P. Maleev¹²⁵, F. Malek⁵⁸, U. Mallik⁶⁶, D. Malon⁶, C. Malone³⁰, S. Maltezos¹⁰, S. Malyukov³², J. Mamuzic¹⁷⁰, G. Mancini⁵⁰, I. Mandić⁷⁸, J. Maneira^{128a,128b}, L. Manhaes de Andrade Filho^{26b}, J. Manjarres Ramos⁴⁷, K.H. Mankinen⁸⁴, A. Mann¹⁰², A. Manousos³², B. Mansoulie¹³⁸, J.D. Mansour^{35a}, R. Mantifel⁹⁰, M. Mantoani⁵⁷, S. Manzoni^{94a,94b}, L. Mapelli³², G. Marceca²⁹, L. March⁵², L. Marchese¹²², G. Marchiori⁸³, M. Marcisovsky¹²⁹, M. Marjanovic³⁷, D.E. Marley⁹², F. Marroquim^{26a}, S.P. Marsden⁸⁷, Z. Marshall¹⁶, M.U.F. Martensson¹⁶⁸, S. Marti-Garcia¹⁷⁰, C.B. Martin¹¹³, T.A. Martin¹⁷³, V.J. Martin⁴⁹, B. Martin dit Latour¹⁵, M. Martinez^{13,v}, V.I. Martinez Outschoorn¹⁶⁹, S. Martin-Haugh¹³³, V.S. Martoiu^{28b}, A.C. Martyniuk⁸¹, A. Marzin³², L. Masetti⁸⁶, T. Mashimo¹⁵⁷, R. Mashinistov⁹⁸, J. Masik⁸⁷, A.L. Maslennikov^{111,c}, L. Massa^{135a,135b}, P. Mastrandrea⁵, A. Mastroberardino^{40a,40b}, T. Masubuchi¹⁵⁷, P. Mättig¹⁷⁸, J. Maurer^{28b}, S.J. Maxfield⁷⁷, D.A. Maximov^{111,c}, R. Mazini¹⁵³, I. Maznas¹⁵⁶, S.M. Mazza^{94a,94b}, N.C. Mc Fadden¹⁰⁷, G. Mc Goldrick¹⁶¹, S.P. Mc Kee⁹², A. McCarn⁹², R.L. McCarthy¹⁵⁰, T.G. McCarthy¹⁰³, L.I. McClymont⁸¹, E.F. McDonald⁹¹, J.A. Mcfayden³², G. Mchedlidze⁵⁷, S.J. McMahon¹³³, P.C. McNamara⁹¹, C.J. McNicol¹⁷³, R.A. McPherson^{172,o}, S. Meehan¹⁴⁰, T.J. Megy⁵¹, S. Mehlhase¹⁰², A. Mehta⁷⁷, T. Meideck⁵⁸, K. Meier^{60a}, B. Meirose⁴⁴, D. Melini^{170,ai}, B.R. Mellado Garcia^{147c}, J.D. Mellenthin⁵⁷, M. Melo^{146a}, F. Meloni¹⁸, A. Melzer²³, S.B. Menary⁸⁷, L. Meng⁷⁷, X.T. Meng⁹², A. Mengarelli^{22a,22b}, S. Menke¹⁰³, E. Meoni^{40a,40b}, S. Mergelmeyer¹⁷, C. Merlassino¹⁸, P. Mermod⁵², L. Merola^{106a,106b}, C. Meroni^{94a}, F.S. Merritt³³, A. Messina^{134a,134b}, J. Metcalfe⁶, A.S. Mete¹⁶⁶, C. Meyer¹²⁴, J-P. Meyer¹³⁸, J. Meyer¹⁰⁹, H. Meyer Zu Theenhausen^{60a}, F. Miano¹⁵¹, R.P. Middleton¹³³, S. Miglioranzi^{53a,53b}, L. Mijović⁴⁹, G. Mikenberg¹⁷⁵, M. Mikestikova¹²⁹, M. Mikuž⁷⁸, M. Milesi⁹¹, A. Milic¹⁶¹, D.A. Millar⁷⁹, D.W. Miller³³, C. Mills⁴⁹, A. Milov¹⁷⁵, D.A. Milstead^{148a,148b}, A.A. Minaenko¹³², Y. Minami¹⁵⁷, I.A. Minashvili⁶⁸, A.I. Mincer¹¹², B. Mindur^{41a}, M. Mineev⁶⁸, Y. Minegishi¹⁵⁷, Y. Ming¹⁷⁶, L.M. Mir¹³, K.P. Mistry¹²⁴, T. Mitani¹⁷⁴, J. Mitrevski¹⁰², V.A. Mitsou¹⁷⁰, A. Miucci¹⁸, P.S. Miyagawa¹⁴¹, A. Mizukami⁶⁹, J.U. Mjörnmark⁸⁴, T. Mkrtchyan¹⁸⁰, M. Mlynarikova¹³¹, T. Moa^{148a,148b}, K. Mochizuki⁹⁷, P. Mogg⁵¹, S. Mohapatra³⁸, S. Molander^{148a,148b}, R. Moles-Valls²³, M.C. Mondragon⁹³, K. Mönig⁴⁵, J. Monk³⁹, E. Monnier⁸⁸, A. Montalbano¹⁵⁰, J. Montejo Berlingen³², F. Monticelli⁷⁴, S. Monzani^{94a,94b}, R.W. Moore³, N. Morange¹¹⁹, D. Moreno²¹, M. Moreno Llacer³², P. Morettini^{53a}, S. Morgenstern³²,

D. Mori ¹⁴⁴, T. Mori ¹⁵⁷, M. Morii ⁵⁹, M. Morinaga ¹⁷⁴, V. Morisbak ¹²¹, A.K. Morley ³², G. Mornacchi ³², J.D. Morris ⁷⁹, L. Morvaj ¹⁵⁰, P. Moschovakos ¹⁰, M. Mosidze ^{54b}, H.J. Moss ¹⁴¹, J. Moss ^{145,aj}, K. Motohashi ¹⁵⁹, R. Mount ¹⁴⁵, E. Mountricha ²⁷, E.J.W. Moyse ⁸⁹, S. Muanza ⁸⁸, F. Mueller ¹⁰³, J. Mueller ¹²⁷, R.S.P. Mueller ¹⁰², D. Muenstermann ⁷⁵, P. Mullen ⁵⁶, G.A. Mullier ¹⁸, F.J. Munoz Sanchez ⁸⁷, W.J. Murray ^{173,133}, H. Musheghyan ³², M. Muškinja ⁷⁸, A.G. Myagkov ^{132,ak}, M. Myska ¹³⁰, B.P. Nachman ¹⁶, O. Nackenhorst ⁵², K. Nagai ¹²², R. Nagai ^{69,ad}, K. Nagano ⁶⁹, Y. Nagasaka ⁶¹, K. Nagata ¹⁶⁴, M. Nagel ⁵¹, E. Nagy ⁸⁸, A.M. Nairz ³², Y. Nakahama ¹⁰⁵, K. Nakamura ⁶⁹, T. Nakamura ¹⁵⁷, I. Nakano ¹¹⁴, R.F. Naranjo Garcia ⁴⁵, R. Narayan ¹¹, D.I. Narrias Villar ^{60a}, I. Naryshkin ¹²⁵, T. Naumann ⁴⁵, G. Navarro ²¹, R. Nayyar ⁷, H.A. Neal ⁹², P.Yu. Nechaeva ⁹⁸, T.J. Neep ¹³⁸, A. Negri ^{123a,123b}, M. Negrini ^{22a}, S. Nektarijevic ¹⁰⁸, C. Nellist ¹¹⁹, A. Nelson ¹⁶⁶, M.E. Nelson ¹²², S. Nemecek ¹²⁹, P. Nemethy ¹¹², M. Nessi ^{32,al}, M.S. Neubauer ¹⁶⁹, M. Neumann ¹⁷⁸, P.R. Newman ¹⁹, T.Y. Ng ^{62c}, T. Nguyen Manh ⁹⁷, R.B. Nickerson ¹²², R. Nicolaïdou ¹³⁸, J. Nielsen ¹³⁹, V. Nikolaenko ^{132,ak}, I. Nikolic-Audit ⁸³, K. Nikolopoulos ¹⁹, J.K. Nilsen ¹²¹, P. Nilsson ²⁷, Y. Ninomiya ¹⁵⁷, A. Nisati ^{134a}, N. Nishu ^{36c}, R. Nisius ¹⁰³, I. Nitsche ⁴⁶, T. Nitta ¹⁷⁴, T. Nobe ¹⁵⁷, Y. Noguchi ⁷¹, M. Nomachi ¹²⁰, I. Nomidis ³¹, M.A. Nomura ²⁷, T. Nooney ⁷⁹, M. Nordberg ³², N. Norjoharuddeen ¹²², O. Novgorodova ⁴⁷, S. Nowak ¹⁰³, M. Nozaki ⁶⁹, L. Nozka ¹¹⁷, K. Ntekas ¹⁶⁶, E. Nurse ⁸¹, F. Nuti ⁹¹, K. O'Connor ²⁵, D.C. O'Neil ¹⁴⁴, A.A. O'Rourke ⁴⁵, V. O'Shea ⁵⁶, F.G. Oakham ^{31,d}, H. Oberlack ¹⁰³, T. Obermann ²³, J. Ocariz ⁸³, A. Ochi ⁷⁰, I. Ochoa ³⁸, J.P. Ochoa-Ricoux ^{34a}, S. Oda ⁷³, S. Odaka ⁶⁹, A. Oh ⁸⁷, S.H. Oh ⁴⁸, C.C. Ohm ¹⁶, H. Ohman ¹⁶⁸, H. Oide ^{53a,53b}, H. Okawa ¹⁶⁴, Y. Okumura ¹⁵⁷, T. Okuyama ⁶⁹, A. Olariu ^{28b}, L.F. Oleiro Seabra ^{128a}, S.A. Olivares Pino ^{34a}, D. Oliveira Damazio ²⁷, A. Olszewski ⁴², J. Olszowska ⁴², A. Onofre ^{128a,128e}, K. Onogi ¹⁰⁵, P.U.E. Onyisi ^{11,z}, H. Oppen ¹²¹, M.J. Oreglia ³³, Y. Oren ¹⁵⁵, D. Orestano ^{136a,136b}, N. Orlando ^{62b}, R.S. Orr ¹⁶¹, B. Osculati ^{53a,53b,*}, R. Ospanov ^{36a}, G. Otero y Garzon ²⁹, H. Otono ⁷³, M. Ouchrif ^{137d}, F. Ould-Saada ¹²¹, A. Ouraou ¹³⁸, K.P. Oussoren ¹⁰⁹, Q. Ouyang ^{35a}, M. Owen ⁵⁶, R.E. Owen ¹⁹, V.E. Ozcan ^{20a}, N. Ozturk ⁸, K. Pachal ¹⁴⁴, A. Pacheco Pages ¹³, L. Pacheco Rodriguez ¹³⁸, C. Padilla Aranda ¹³, S. Pagan Griso ¹⁶, M. Paganini ¹⁷⁹, F. Paige ²⁷, G. Palacino ⁶⁴, S. Palazzo ^{40a,40b}, S. Palestini ³², M. Palka ^{41b}, D. Pallin ³⁷, E.St. Panagiotopoulou ¹⁰, I. Panagoulas ¹⁰, C.E. Pandini ^{126a,126b}, J.G. Panduro Vazquez ⁸⁰, P. Pani ³², S. Panitkin ²⁷, D. Pantea ^{28b}, L. Paolozzi ⁵², Th.D. Papadopolou ¹⁰, K. Papageorgiou ^{9,s}, A. Paramonov ⁶, D. Paredes Hernandez ¹⁷⁹, A.J. Parker ⁷⁵, M.A. Parker ³⁰, K.A. Parker ⁴⁵, F. Parodi ^{53a,53b}, J.A. Parsons ³⁸, U. Parzefall ⁵¹, V.R. Pascuzzi ¹⁶¹, J.M. Pasner ¹³⁹, E. Pasqualucci ^{134a}, S. Passaggio ^{53a}, Fr. Pastore ⁸⁰, S. Pataria ⁸⁶, J.R. Pater ⁸⁷, T. Pauly ³², B. Pearson ¹⁰³, S. Pedraza Lopez ¹⁷⁰, R. Pedro ^{128a,128b}, S.V. Peleganchuk ^{111,c}, O. Penc ¹²⁹, C. Peng ^{35a}, H. Peng ^{36a}, J. Penwell ⁶⁴, B.S. Peralva ^{26b}, M.M. Perego ¹³⁸, D.V. Perepelitsa ²⁷, F. Peri ¹⁷, L. Perini ^{94a,94b}, H. Pernegger ³², S. Perrella ^{106a,106b}, R. Peschke ⁴⁵, V.D. Peshekhonov ^{68,*}, K. Peters ⁴⁵, R.F.Y. Peters ⁸⁷, B.A. Petersen ³², T.C. Petersen ³⁹, E. Petit ⁵⁸, A. Petridis ¹, C. Petridou ¹⁵⁶, P. Petroff ¹¹⁹, E. Petrolo ^{134a}, M. Petrov ¹²², F. Petrucci ^{136a,136b}, N.E. Pettersson ⁸⁹, A. Peyaud ¹³⁸, R. Pezoa ^{34b}, F.H. Phillips ⁹³, P.W. Phillips ¹³³, G. Piacquadio ¹⁵⁰, E. Pianori ¹⁷³, A. Picazio ⁸⁹, E. Piccaro ⁷⁹, M.A. Pickering ¹²², R. Piegaia ²⁹, J.E. Pilcher ³³, A.D. Pilkington ⁸⁷, A.W.J. Pin ⁸⁷, M. Pinamonti ^{135a,135b}, J.L. Pinfold ³, H. Pirumov ⁴⁵, M. Pitt ¹⁷⁵, L. Plazak ^{146a}, M.-A. Pleier ²⁷, V. Pleskot ⁸⁶, E. Plotnikova ⁶⁸, D. Pluth ⁶⁷, P. Podberezko ¹¹¹, R. Poettgen ⁸⁴, R. Poggi ^{123a,123b}, L. Poggioli ¹¹⁹, I. Pogrebnyak ⁹³, D. Pohl ²³, G. Polesello ^{123a}, A. Poley ⁴⁵, A. Policicchio ^{40a,40b}, R. Polifka ³², A. Polini ^{22a}, C.S. Pollard ⁵⁶, V. Polychronakos ²⁷, K. Pommès ³², D. Ponomarenko ¹⁰⁰, L. Pontecorvo ^{134a}, G.A. Popeneciu ^{28d}, S. Pospisil ¹³⁰, K. Potamianos ¹⁶, I.N. Potrap ⁶⁸, C.J. Potter ³⁰, T. Poulsen ⁸⁴, J. Poveda ³², M.E. Pozo Astigarraga ³², P. Pralavorio ⁸⁸, A. Pranko ¹⁶, S. Prell ⁶⁷, D. Price ⁸⁷, M. Primavera ^{76a}, S. Prince ⁹⁰, N. Proklova ¹⁰⁰, K. Prokofiev ^{62c}, F. Prokoshin ^{34b}, S. Protopopescu ²⁷, J. Proudfoot ⁶, M. Przybycien ^{41a}, A. Puri ¹⁶⁹, P. Puzo ¹¹⁹, J. Qian ⁹², G. Qin ⁵⁶, Y. Qin ⁸⁷, A. Quadt ⁵⁷, M. Queitsch-Maitland ⁴⁵, D. Quilty ⁵⁶, S. Raddum ¹²¹, V. Radeka ²⁷, V. Radescu ¹²², S.K. Radhakrishnan ¹⁵⁰, P. Radloff ¹¹⁸, P. Rados ⁹¹, F. Ragusa ^{94a,94b}, G. Rahal ¹⁸¹, J.A. Raine ⁸⁷, S. Rajagopalan ²⁷, C. Rangel-Smith ¹⁶⁸, T. Rashid ¹¹⁹, S. Raspopov ⁵, M.G. Ratti ^{94a,94b}, D.M. Rauch ⁴⁵, F. Rauscher ¹⁰², S. Rave ⁸⁶, I. Ravinovich ¹⁷⁵, J.H. Rawling ⁸⁷, M. Raymond ³², A.L. Read ¹²¹, N.P. Readoff ⁵⁸, M. Reale ^{76a,76b}, D.M. Rebuzzi ^{123a,123b}, A. Redelbach ¹⁷⁷, G. Redlinger ²⁷, R. Reece ¹³⁹, R.G. Reed ^{147c}, K. Reeves ⁴⁴, L. Rehnisch ¹⁷, J. Reichert ¹²⁴, A. Reiss ⁸⁶, C. Rembser ³², H. Ren ^{35a}, M. Rescigno ^{134a}, S. Resconi ^{94a}, E.D. Resseguie ¹²⁴, S. Rettie ¹⁷¹, E. Reynolds ¹⁹, O.L. Rezanova ^{111,c}, P. Reznicek ¹³¹, R. Rezvani ⁹⁷, R. Richter ¹⁰³, S. Richter ⁸¹,

E. Richter-Was^{41b}, O. Ricken²³, M. Ridel⁸³, P. Rieck¹⁰³, C.J. Riegel¹⁷⁸, J. Rieger⁵⁷, O. Rifki¹¹⁵, M. Rijssenbeek¹⁵⁰, A. Rimoldi^{123a,123b}, M. Rimoldi¹⁸, L. Rinaldi^{22a}, G. Ripellino¹⁴⁹, B. Ristić³², E. Ritsch³², I. Riu¹³, F. Rizatdinova¹¹⁶, E. Rizvi⁷⁹, C. Rizzi¹³, R.T. Roberts⁸⁷, S.H. Robertson^{90,o}, A. Robichaud-Veronneau⁹⁰, D. Robinson³⁰, J.E.M. Robinson⁴⁵, A. Robson⁵⁶, E. Rocco⁸⁶, C. Roda^{126a,126b}, Y. Rodina^{88,am}, S. Rodriguez Bosca¹⁷⁰, A. Rodriguez Perez¹³, D. Rodriguez Rodriguez¹⁷⁰, S. Roe³², C.S. Rogan⁵⁹, O. Røhne¹²¹, J. Roloff⁵⁹, A. Romaniouk¹⁰⁰, M. Romano^{22a,22b}, S.M. Romano Saez³⁷, E. Romero Adam¹⁷⁰, N. Rompotis⁷⁷, M. Ronzani⁵¹, L. Roos⁸³, S. Rosati^{134a}, K. Rosbach⁵¹, P. Rose¹³⁹, N.-A. Rosien⁵⁷, E. Rossi^{106a,106b}, L.P. Rossi^{53a}, J.H.N. Rosten³⁰, R. Rosten¹⁴⁰, M. Rotaru^{28b}, J. Rothberg¹⁴⁰, D. Rousseau¹¹⁹, A. Rozanov⁸⁸, Y. Rozen¹⁵⁴, X. Ruan^{147c}, F. Rubbo¹⁴⁵, F. Rühr⁵¹, A. Ruiz-Martinez³¹, Z. Rurikova⁵¹, N.A. Rusakovich⁶⁸, H.L. Russell⁹⁰, J.P. Rutherford⁷, N. Ruthmann³², Y.F. Ryabov¹²⁵, M. Rybar¹⁶⁹, G. Rybkin¹¹⁹, S. Ryu⁶, A. Ryzhov¹³², G.F. Rzehorz⁵⁷, A.F. Saavedra¹⁵², G. Sabato¹⁰⁹, S. Sacerdoti²⁹, H.F.-W. Sadrozinski¹³⁹, R. Sadykov⁶⁸, F. Safai Tehrani^{134a}, P. Saha¹¹⁰, M. Sahinsoy^{60a}, M. Saimpert⁴⁵, M. Saito¹⁵⁷, T. Saito¹⁵⁷, H. Sakamoto¹⁵⁷, Y. Sakurai¹⁷⁴, G. Salamanna^{136a,136b}, J.E. Salazar Loyola^{34b}, D. Salek¹⁰⁹, P.H. Sales De Bruin¹⁶⁸, D. Salihagic¹⁰³, A. Salnikov¹⁴⁵, J. Salt¹⁷⁰, D. Salvatore^{40a,40b}, F. Salvatore¹⁵¹, A. Salvucci^{62a,62b,62c}, A. Salzburger³², D. Sammel⁵¹, D. Sampsonidis¹⁵⁶, D. Sampsonidou¹⁵⁶, J. Sánchez¹⁷⁰, V. Sanchez Martinez¹⁷⁰, A. Sanchez Pineda^{167a,167c}, H. Sandaker¹²¹, R.L. Sandbach⁷⁹, C.O. Sander⁴⁵, M. Sandhoff¹⁷⁸, C. Sandoval²¹, D.P.C. Sankey¹³³, M. Sannino^{53a,53b}, Y. Sano¹⁰⁵, A. Sansoni⁵⁰, C. Santoni³⁷, H. Santos^{128a}, I. Santoyo Castillo¹⁵¹, A. Sapronov⁶⁸, J.G. Saraiva^{128a,128d}, B. Sarrazin²³, O. Sasaki⁶⁹, K. Sato¹⁶⁴, E. Sauvan⁵, G. Savage⁸⁰, P. Savard^{161,d}, N. Savic¹⁰³, C. Sawyer¹³³, L. Sawyer^{82,u}, J. Saxon³³, C. Sbarra^{22a}, A. Sbrizzi^{22a,22b}, T. Scanlon⁸¹, D.A. Scannicchio¹⁶⁶, J. Schaarschmidt¹⁴⁰, P. Schacht¹⁰³, B.M. Schachtner¹⁰², D. Schaefer³², L. Schaefer¹²⁴, R. Schaefer⁴⁵, J. Schaeffer⁸⁶, S. Schaepe²³, S. Schaetzel^{60b}, U. Schäfer⁸⁶, A.C. Schaffer¹¹⁹, D. Schaile¹⁰², R.D. Schamberger¹⁵⁰, V.A. Schegelsky¹²⁵, D. Scheirich¹³¹, M. Schernau¹⁶⁶, C. Schiavi^{53a,53b}, S. Schier¹³⁹, L.K. Schildgen²³, C. Schillo⁵¹, M. Schioppa^{40a,40b}, S. Schlenker³², K.R. Schmidt-Sommerfeld¹⁰³, K. Schmieden³², C. Schmitt⁸⁶, S. Schmitt⁴⁵, S. Schmitz⁸⁶, U. Schnoor⁵¹, L. Schoeffel¹³⁸, A. Schoening^{60b}, B.D. Schoenrock⁹³, E. Schopf²³, M. Schott⁸⁶, J.F.P. Schouwenberg¹⁰⁸, J. Schovancova³², S. Schramm⁵², N. Schuh⁸⁶, A. Schulte⁸⁶, M.J. Schultens²³, H.-C. Schultz-Coulon^{60a}, H. Schulz¹⁷, M. Schumacher⁵¹, B.A. Schumm¹³⁹, Ph. Schune¹³⁸, A. Schwartzman¹⁴⁵, T.A. Schwarz⁹², H. Schweiger⁸⁷, Ph. Schwemling¹³⁸, R. Schwienhorst⁹³, J. Schwindling¹³⁸, A. Sciandra²³, G. Sciolla²⁵, M. Scornajenghi^{40a,40b}, F. Scuri^{126a,126b}, F. Scutti⁹¹, J. Searcy⁹², P. Seema²³, S.C. Seidel¹⁰⁷, A. Seiden¹³⁹, J.M. Seixas^{26a}, G. Sekhniaidze^{106a}, K. Sekhon⁹², S.J. Sekula⁴³, N. Semprini-Cesari^{22a,22b}, S. Senkin³⁷, C. Serfon¹²¹, L. Serin¹¹⁹, L. Serkin^{167a,167b}, M. Sessa^{136a,136b}, R. Seuster¹⁷², H. Severini¹¹⁵, T. Sfiligoi⁷⁸, F. Sforza¹⁶⁵, A. Sfyrla⁵², E. Shabalina⁵⁷, N.W. Shaikh^{148a,148b}, L.Y. Shan^{35a}, R. Shang¹⁶⁹, J.T. Shank²⁴, M. Shapiro¹⁶, P.B. Shatalov⁹⁹, K. Shaw^{167a,167b}, S.M. Shaw⁸⁷, A. Shcherbakova^{148a,148b}, C.Y. Shehu¹⁵¹, Y. Shen¹¹⁵, N. Sherafati³¹, P. Sherwood⁸¹, L. Shi^{153,an}, S. Shimizu⁷⁰, C.O. Shimmin¹⁷⁹, M. Shimojima¹⁰⁴, I.P.J. Shipsey¹²², S. Shirabe⁷³, M. Shiyakova^{68,ao}, J. Shlomi¹⁷⁵, A. Shmeleva⁹⁸, D. Shoaleh Saadi⁹⁷, M.J. Shochet³³, S. Shojaii^{94a}, D.R. Shope¹¹⁵, S. Shrestha¹¹³, E. Shulga¹⁰⁰, M.A. Shupe⁷, P. Sicho¹²⁹, A.M. Sickles¹⁶⁹, P.E. Sidebo¹⁴⁹, E. Sideras Haddad^{147c}, O. Sidiropoulou¹⁷⁷, A. Sidoti^{22a,22b}, F. Siegert⁴⁷, Dj. Sijacki¹⁴, J. Silva^{128a,128d}, S.B. Silverstein^{148a}, V. Simak¹³⁰, Lj. Simic¹⁴, S. Simion¹¹⁹, E. Simioni⁸⁶, B. Simmons⁸¹, M. Simon⁸⁶, P. Sinervo¹⁶¹, N.B. Sinev¹¹⁸, M. Sioli^{22a,22b}, G. Siragusa¹⁷⁷, I. Siral⁹², S.Yu. Sivoklokov¹⁰¹, J. Sjölin^{148a,148b}, M.B. Skinner⁷⁵, P. Skubic¹¹⁵, M. Slater¹⁹, T. Slavicek¹³⁰, M. Slawinska⁴², K. Sliwa¹⁶⁵, R. Slovak¹³¹, V. Smakhtin¹⁷⁵, B.H. Smart⁵, J. Smiesko^{146a}, N. Smirnov¹⁰⁰, S.Yu. Smirnov¹⁰⁰, Y. Smirnov¹⁰⁰, L.N. Smirnova^{101,ap}, O. Smirnova⁸⁴, J.W. Smith⁵⁷, M.N.K. Smith³⁸, R.W. Smith³⁸, M. Smizanska⁷⁵, K. Smolek¹³⁰, A.A. Snesarev⁹⁸, I.M. Snyder¹¹⁸, S. Snyder²⁷, R. Sobie^{172,o}, F. Socher⁴⁷, A. Soffer¹⁵⁵, A. Søgaard⁴⁹, D.A. Soh¹⁵³, G. Sokhrannyi⁷⁸, C.A. Solans Sanchez³², M. Solar¹³⁰, E.Yu. Soldatov¹⁰⁰, U. Soldevila¹⁷⁰, A.A. Solodkov¹³², A. Soloshenko⁶⁸, O.V. Solovyanov¹³², V. Solovyev¹²⁵, P. Sommer⁵¹, H. Son¹⁶⁵, A. Sopczak¹³⁰, D. Sosa^{60b}, C.L. Sotiropoulou^{126a,126b}, R. Soualah^{167a,167c}, A.M. Soukharev^{111,c}, D. South⁴⁵, B.C. Sowden⁸⁰, S. Spagnolo^{76a,76b}, M. Spalla^{126a,126b}, M. Spangenberg¹⁷³, F. Spanò⁸⁰, D. Sperlich¹⁷, F. Spettel¹⁰³, T.M. Spieker^{60a}, R. Spighi^{22a}, G. Spigo³², L.A. Spiller⁹¹, M. Spousta¹³¹, R.D. St. Denis^{56,*}, A. Stabile^{94a}, R. Stamen^{60a}, S. Stamm¹⁷, E. Stanecka⁴², R.W. Stanek⁶, C. Stanescu^{136a}, M.M. Stanitzki⁴⁵,

B.S. Stapf¹⁰⁹, S. Stapnes¹²¹, E.A. Starchenko¹³², G.H. Stark³³, J. Stark⁵⁸, S.H. Stark³⁹, P. Staroba¹²⁹, P. Starovoitov^{60a}, S. Stärz³², R. Staszewski⁴², P. Steinberg²⁷, B. Stelzer¹⁴⁴, H.J. Stelzer³², O. Stelzer-Chilton^{163a}, H. Stenzel⁵⁵, G.A. Stewart⁵⁶, M.C. Stockton¹¹⁸, M. Stoebe⁹⁰, G. Stoicea^{28b}, P. Stolte⁵⁷, S. Stonjek¹⁰³, A.R. Stradling⁸, A. Straessner⁴⁷, M.E. Stramaglia¹⁸, J. Strandberg¹⁴⁹, S. Strandberg^{148a,148b}, M. Strauss¹¹⁵, P. Strizenec^{146b}, R. Ströhmer¹⁷⁷, D.M. Strom¹¹⁸, R. Stroyanowski⁴³, A. Strubig⁴⁹, S.A. Stucci²⁷, B. Stugu¹⁵, N.A. Styles⁴⁵, D. Su¹⁴⁵, J. Su¹²⁷, S. Suchek^{60a}, Y. Sugaya¹²⁰, M. Suk¹³⁰, V.V. Sulin⁹⁸, DMS Sultan^{162a,162b}, S. Sultansoy^{4c}, T. Sumida⁷¹, S. Sun⁵⁹, X. Sun³, K. Suruliz¹⁵¹, C.J.E. Suster¹⁵², M.R. Sutton¹⁵¹, S. Suzuki⁶⁹, M. Svatos¹²⁹, M. Swiatlowski³³, S.P. Swift², I. Sykora^{146a}, T. Sykora¹³¹, D. Ta⁵¹, K. Tackmann⁴⁵, J. Taenzer¹⁵⁵, A. Taffard¹⁶⁶, R. Tafirout^{163a}, E. Tahirovic⁷⁹, N. Taiblum¹⁵⁵, H. Takai²⁷, R. Takashima⁷², E.H. Takasugi¹⁰³, T. Takeshita¹⁴², Y. Takubo⁶⁹, M. Talby⁸⁸, A.A. Talyshchev^{111,c}, J. Tanaka¹⁵⁷, M. Tanaka¹⁵⁹, R. Tanaka¹¹⁹, S. Tanaka⁶⁹, R. Tanioka⁷⁰, B.B. Tannenwald¹¹³, S. Tapia Araya^{34b}, S. Tapprogge⁸⁶, S. Tarem¹⁵⁴, G.F. Tartarelli^{94a}, P. Tas¹³¹, M. Tasevsky¹²⁹, T. Tashiro⁷¹, E. Tassi^{40a,40b}, A. Tavares Delgado^{128a,128b}, Y. Tayalati^{137e}, A.C. Taylor¹⁰⁷, A.J. Taylor⁴⁹, G.N. Taylor⁹¹, P.T.E. Taylor⁹¹, W. Taylor^{163b}, P. Teixeira-Dias⁸⁰, D. Temple¹⁴⁴, H. Ten Kate³², P.K. Teng¹⁵³, J.J. Teoh¹²⁰, F. Tepel¹⁷⁸, S. Terada⁶⁹, K. Terashi¹⁵⁷, J. Terron⁸⁵, S. Terzo¹³, M. Testa⁵⁰, R.J. Teuscher^{161,o}, T. Theveneaux-Pelzer⁸⁸, F. Thiele³⁹, J.P. Thomas¹⁹, J. Thomas-Wilsker⁸⁰, P.D. Thompson¹⁹, A.S. Thompson⁵⁶, L.A. Thomsen¹⁷⁹, E. Thomson¹²⁴, M.J. Tibbetts¹⁶, R.E. Ticse Torres⁸⁸, V.O. Tikhomirov^{98,aq}, Yu.A. Tikhonov^{111,c}, S. Timoshenko¹⁰⁰, P. Tipton¹⁷⁹, S. Tisserant⁸⁸, K. Todome¹⁵⁹, S. Todorova-Nova⁵, S. Todt⁴⁷, J. Tojo⁷³, S. Tokár^{146a}, K. Tokushuku⁶⁹, E. Tolley⁵⁹, L. Tomlinson⁸⁷, M. Tomoto¹⁰⁵, L. Tompkins^{145,ar}, K. Toms¹⁰⁷, B. Tong⁵⁹, P. Tornambe⁵¹, E. Torrence¹¹⁸, H. Torres⁴⁷, E. Torró Pastor¹⁴⁰, J. Toth^{88,as}, F. Touchard⁸⁸, D.R. Tovey¹⁴¹, C.J. Treado¹¹², T. Trefzger¹⁷⁷, F. Tresoldi¹⁵¹, A. Tricoli²⁷, I.M. Trigger^{163a}, S. Trincaz-Duvold⁸³, M.F. Tripiana¹³, W. Trischuk¹⁶¹, B. Trocmé⁵⁸, A. Trofymov⁴⁵, C. Troncon^{94a}, M. Trotter-McDonald¹⁶, M. Trovatelli¹⁷², L. Truong^{147b}, M. Trzebinski⁴², A. Trzupek⁴², K.W. Tsang^{62a}, J.C.-L. Tseng¹²², P.V. Tsiarashka⁹⁵, G. Tsipolitis¹⁰, N. Tsirintanis⁹, S. Tsiskaridze¹³, V. Tsiskaridze⁵¹, E.G. Tskhadadze^{54a}, K.M. Tsui^{62a}, I.I. Tsukerman⁹⁹, V. Tsulaia¹⁶, S. Tsuno⁶⁹, D. Tsybychev¹⁵⁰, Y. Tu^{62b}, A. Tudorache^{28b}, V. Tudorache^{28b}, T.T. Tulbure^{28a}, A.N. Tuna⁵⁹, S.A. Tupputi^{22a,22b}, S. Turchikhin⁶⁸, D. Turgeman¹⁷⁵, I. Turk Cakir^{4b,at}, R. Turra^{94a}, P.M. Tuts³⁸, G. Uccielli^{22a,22b}, I. Ueda⁶⁹, M. Ughetto^{148a,148b}, F. Ukegawa¹⁶⁴, G. Unal³², A. Undrus²⁷, G. Unel¹⁶⁶, F.C. Ungaro⁹¹, Y. Unno⁶⁹, C. Unverdorben¹⁰², J. Urban^{146b}, P. Urquijo⁹¹, P. Urrejola⁸⁶, G. Usai⁸, J. Usui⁶⁹, L. Vacavant⁸⁸, V. Vacek¹³⁰, B. Vachon⁹⁰, K.O.H. Vadla¹²¹, A. Vaidya⁸¹, C. Valderanis¹⁰², E. Valdes Santurio^{148a,148b}, M. Valente⁵², S. Valentini^{22a,22b}, A. Valero¹⁷⁰, L. Valéry¹³, S. Valkar¹³¹, A. Vallier⁵, J.A. Valls Ferrer¹⁷⁰, W. Van Den Wollenberg¹⁰⁹, H. van der Graaf¹⁰⁹, P. van Gemmeren⁶, J. Van Nieuwkoop¹⁴⁴, I. van Vulpen¹⁰⁹, M.C. van Woerden¹⁰⁹, M. Vanadia^{135a,135b}, W. Vandelli³², A. Vaniachine¹⁶⁰, P. Vankov¹⁰⁹, G. Vardanyan¹⁸⁰, R. Vari^{134a}, E.W. Varnes⁷, C. Varni^{53a,53b}, T. Varol⁴³, D. Varouchas¹¹⁹, A. Vartapetian⁸, K.E. Varvell¹⁵², J.G. Vasquez¹⁷⁹, G.A. Vasquez^{34b}, F. Vazeille³⁷, T. Vazquez Schroeder⁹⁰, J. Veatch⁵⁷, V. Veeraraghavan⁷, L.M. Veloce¹⁶¹, F. Veloso^{128a,128c}, S. Veneziano^{134a}, A. Ventura^{76a,76b}, M. Venturi¹⁷², N. Venturi³², A. Venturini²⁵, V. Vercesi^{123a}, M. Verducci^{136a,136b}, W. Verkerke¹⁰⁹, A.T. Vermeulen¹⁰⁹, J.C. Vermeulen¹⁰⁹, M.C. Vetterli^{144,d}, N. Viaux Maira^{34b}, O. Viazlo⁸⁴, I. Vichou^{169,*}, T. Vickey¹⁴¹, O.E. Vickey Boeriu¹⁴¹, G.H.A. Viehhauser¹²², S. Viel¹⁶, L. Vigani¹²², M. Villa^{22a,22b}, M. Villaplana Perez^{94a,94b}, E. Vilucchi⁵⁰, M.G. Vincet³¹, V.B. Vinogradov⁶⁸, A. Vishwakarma⁴⁵, C. Vittori^{22a,22b}, I. Vivarelli¹⁵¹, S. Vlachos¹⁰, M. Vogel¹⁷⁸, P. Vokac¹³⁰, G. Volpi¹³, H. von der Schmitt¹⁰³, E. von Toerne²³, V. Vorobel¹³¹, K. Vorobev¹⁰⁰, M. Vos¹⁷⁰, R. Voss³², J.H. Vosseveld⁷⁷, N. Vranjes¹⁴, M. Vranjes Milosavljevic¹⁴, V. Vrba¹³⁰, M. Vreeswijk¹⁰⁹, R. Vuillermet³², I. Vukotic³³, P. Wagner²³, W. Wagner¹⁷⁸, J. Wagner-Kuhr¹⁰², H. Wahlberg⁷⁴, S. Wahrmond⁴⁷, J. Walder⁷⁵, R. Walker¹⁰², W. Walkowiak¹⁴³, V. Wallangen^{148a,148b}, C. Wang^{35b}, C. Wang^{36b,au}, F. Wang¹⁷⁶, H. Wang¹⁶, H. Wang³, J. Wang⁴⁵, J. Wang¹⁵², Q. Wang¹¹⁵, R. Wang⁶, S.M. Wang¹⁵³, T. Wang³⁸, W. Wang^{153,av}, W. Wang^{36a}, Z. Wang^{36c}, C. Wanotayaroj¹¹⁸, A. Warburton⁹⁰, C.P. Ward³⁰, D.R. Wardrope⁸¹, A. Washbrook⁴⁹, P.M. Watkins¹⁹, A.T. Watson¹⁹, M.F. Watson¹⁹, G. Watts¹⁴⁰, S. Watts⁸⁷, B.M. Waugh⁸¹, A.F. Webb¹¹, S. Webb⁸⁶, M.S. Weber¹⁸, S.W. Weber¹⁷⁷, S.A. Weber³¹, J.S. Webster⁶, A.R. Weidberg¹²², B. Weinert⁶⁴, J. Weingarten⁵⁷, M. Weirich⁸⁶, C. Weiser⁵¹, H. Weits¹⁰⁹, P.S. Wells³², T. Wenaus²⁷, T. Wengler³², S. Wenig³², N. Wermes²³, M.D. Werner⁶⁷, P. Werner³²,

M. Wessels^{60a}, T.D. Weston¹⁸, K. Whalen¹¹⁸, N.L. Whallon¹⁴⁰, A.M. Wharton⁷⁵, A.S. White⁹²,
 A. White⁸, M.J. White¹, R. White^{34b}, D. Whiteson¹⁶⁶, B.W. Whitmore⁷⁵, F.J. Wickens¹³³,
 W. Wiedenmann¹⁷⁶, M. Wielers¹³³, C. Wiglesworth³⁹, L.A.M. Wiik-Fuchs⁵¹, A. Wildauer¹⁰³, F. Wilk⁸⁷,
 H.G. Wilkens³², H.H. Williams¹²⁴, S. Williams¹⁰⁹, C. Willis⁹³, S. Willocq⁸⁹, J.A. Wilson¹⁹,
 I. Wingerter-Seez⁵, E. Winkels¹⁵¹, F. Winklmeier¹¹⁸, O.J. Winston¹⁵¹, B.T. Winter²³, M. Wittgen¹⁴⁵,
 M. Wobisch^{82,u}, T.M.H. Wolf¹⁰⁹, R. Wolff⁸⁸, M.W. Wolter⁴², H. Wolters^{128a,128c}, V.W.S. Wong¹⁷¹,
 S.D. Worm¹⁹, B.K. Wosiek⁴², J. Wotschack³², K.W. Wozniak⁴², M. Wu³³, S.L. Wu¹⁷⁶, X. Wu⁵², Y. Wu⁹²,
 T.R. Wyatt⁸⁷, B.M. Wynne⁴⁹, S. Xella³⁹, Z. Xi⁹², L. Xia^{35c}, D. Xu^{35a}, L. Xu²⁷, T. Xu¹³⁸, B. Yabsley¹⁵²,
 S. Yacoob^{147a}, D. Yamaguchi¹⁵⁹, Y. Yamaguchi¹⁵⁹, A. Yamamoto⁶⁹, S. Yamamoto¹⁵⁷, T. Yamanaka¹⁵⁷,
 F. Yamane⁷⁰, M. Yamatani¹⁵⁷, Y. Yamazaki⁷⁰, Z. Yan²⁴, H. Yang^{36c}, H. Yang¹⁶, Y. Yang¹⁵³, Z. Yang¹⁵,
 W.-M. Yao¹⁶, Y.C. Yap⁸³, Y. Yasu⁶⁹, E. Yatsenko⁵, K.H. Yau Wong²³, J. Ye⁴³, S. Ye²⁷, I. Yeletsikh⁶⁸,
 E. Yigitbasi²⁴, E. Yildirim⁸⁶, K. Yorita¹⁷⁴, K. Yoshihara¹²⁴, C. Young¹⁴⁵, C.J.S. Young³², J. Yu⁸, J. Yu⁶⁷,
 S.P.Y. Yuen²³, I. Yusuff^{30,aw}, B. Zabinski⁴², G. Zacharis¹⁰, R. Zaidan¹³, A.M. Zaitsev^{132,ak},
 N. Zakharchuk⁴⁵, J. Zalieckas¹⁵, A. Zaman¹⁵⁰, S. Zambito⁵⁹, D. Zanzi⁹¹, C. Zeitnitz¹⁷⁸, G. Zemaityte¹²²,
 A. Zemla^{41a}, J.C. Zeng¹⁶⁹, Q. Zeng¹⁴⁵, O. Zenin¹³², T. Ženiš^{146a}, D. Zerwas¹¹⁹, D. Zhang⁹², F. Zhang¹⁷⁶,
 G. Zhang^{36a,ax}, H. Zhang^{35b}, J. Zhang⁶, L. Zhang⁵¹, L. Zhang^{36a}, M. Zhang¹⁶⁹, P. Zhang^{35b}, R. Zhang²³,
 R. Zhang^{36a,au}, X. Zhang^{36b}, Y. Zhang^{35a}, Z. Zhang¹¹⁹, X. Zhao⁴³, Y. Zhao^{36b,ay}, Z. Zhao^{36a},
 A. Zhemchugov⁶⁸, B. Zhou⁹², C. Zhou¹⁷⁶, L. Zhou⁴³, M. Zhou^{35a}, M. Zhou¹⁵⁰, N. Zhou^{35c}, C.G. Zhu^{36b},
 H. Zhu^{35a}, J. Zhu⁹², Y. Zhu^{36a}, X. Zhuang^{35a}, K. Zhukov⁹⁸, A. Zibell¹⁷⁷, D. Zieminska⁶⁴, N.I. Zimine⁶⁸,
 C. Zimmermann⁸⁶, S. Zimmermann⁵¹, Z. Zinonos¹⁰³, M. Zinser⁸⁶, M. Ziolkowski¹⁴³, L. Živković¹⁴,
 G. Zobernig¹⁷⁶, A. Zoccoli^{22a,22b}, R. Zou³³, M. zur Nedden¹⁷, L. Zwalinski³²

¹ Department of Physics, University of Adelaide, Adelaide, Australia

² Physics Department, SUNY Albany, Albany NY, United States

³ Department of Physics, University of Alberta, Edmonton AB, Canada

⁴ (a) Department of Physics, Ankara University, Ankara; (b) Istanbul Aydin University, Istanbul; (c) Division of Physics, TOBB University of Economics and Technology, Ankara, Turkey

⁵ LAPP, CNRS/IN2P3 and Université Savoie Mont Blanc, Annecy-le-Vieux, France

⁶ High Energy Physics Division, Argonne National Laboratory, Argonne IL, United States

⁷ Department of Physics, University of Arizona, Tucson AZ, United States

⁸ Department of Physics, The University of Texas at Arlington, Arlington TX, United States

⁹ Physics Department, National and Kapodistrian University of Athens, Athens, Greece

¹⁰ Physics Department, National Technical University of Athens, Zografou, Greece

¹¹ Department of Physics, The University of Texas at Austin, Austin TX, United States

¹² Institute of Physics, Azerbaijan Academy of Sciences, Baku, Azerbaijan

¹³ Institut de Física d'Altes Energies (IFAE), The Barcelona Institute of Science and Technology, Barcelona, Spain

¹⁴ Institute of Physics, University of Belgrade, Belgrade, Serbia

¹⁵ Department for Physics and Technology, University of Bergen, Bergen, Norway

¹⁶ Physics Division, Lawrence Berkeley National Laboratory and University of California, Berkeley CA, United States

¹⁷ Department of Physics, Humboldt University, Berlin, Germany

¹⁸ Albert Einstein Center for Fundamental Physics and Laboratory for High Energy Physics, University of Bern, Bern, Switzerland

¹⁹ School of Physics and Astronomy, University of Birmingham, Birmingham, United Kingdom

²⁰ (a) Department of Physics, Bogazici University, Istanbul; (b) Department of Physics Engineering, Gaziantep University, Gaziantep; (c) Istanbul Bilgi University, Faculty of Engineering and Natural Sciences, Istanbul; (d) Bahcesehir University, Faculty of Engineering and Natural Sciences, Istanbul, Turkey

²¹ Centro de Investigaciones, Universidad Antonio Narino, Bogota, Colombia

²² (a) INFN Sezione di Bologna; (b) Dipartimento di Fisica e Astronomia, Università di Bologna, Bologna, Italy

²³ Physikalisches Institut, University of Bonn, Bonn, Germany

²⁴ Department of Physics, Boston University, Boston MA, United States

²⁵ Department of Physics, Brandeis University, Waltham MA, United States

²⁶ (a) Universidade Federal do Rio De Janeiro COPPE/EE/IF, Rio de Janeiro; (b) Electrical Circuits Department, Federal University of Juiz de Fora (UFJF), Juiz de Fora; (c) Federal University of Sao Joao del Rei (UFSJ), Sao Joao del Rei; (d) Instituto de Fisica, Universidade de Sao Paulo, Sao Paulo, Brazil

²⁷ Physics Department, Brookhaven National Laboratory, Upton NY, United States

²⁸ (a) Transilvania University of Brasov, Brasov; (b) Horia Hulubei National Institute of Physics and Nuclear Engineering, Bucharest; (c) Department of Physics, Alexandru Ioan Cuza University of Iasi, Iasi; (d) National Institute for Research and Development of Isotopic and Molecular Technologies, Physics Department, Cluj Napoca; (e) University Politehnica Bucharest, Bucharest; (f) West University in Timisoara, Timisoara, Romania

²⁹ Departamento de Física, Universidad de Buenos Aires, Buenos Aires, Argentina

³⁰ Cavendish Laboratory, University of Cambridge, Cambridge, United Kingdom

³¹ Department of Physics, Carleton University, Ottawa ON, Canada

³² CERN, Geneva, Switzerland

³³ Enrico Fermi Institute, University of Chicago, Chicago IL, United States

³⁴ (a) Departamento de Física, Pontificia Universidad Católica de Chile, Santiago; (b) Departamento de Física, Universidad Técnica Federico Santa María, Valparaíso, Chile

³⁵ (a) Institute of High Energy Physics, Chinese Academy of Sciences, Beijing; (b) Department of Physics, Nanjing University, Jiangsu; (c) Physics Department, Tsinghua University, Beijing 100084, China

³⁶ (a) Department of Modern Physics and State Key Laboratory of Particle Detection and Electronics, University of Science and Technology of China, Anhui; (b) School of Physics, Shandong University, Shandong; (c) Department of Physics and Astronomy, Key Laboratory for Particle Physics, Astrophysics and Cosmology, Ministry of Education, Shanghai Key Laboratory for Particle Physics and Cosmology, Shanghai Jiao Tong University, Shanghai, China

³⁷ Université Clermont Auvergne, CNRS/IN2P3, LPC, Clermont-Ferrand, France

³⁸ Nevis Laboratory, Columbia University, Irvington NY, United States

³⁹ Niels Bohr Institute, University of Copenhagen, Copenhagen, Denmark

- ⁴⁰ ^(a) INFN Gruppo Collegato di Cosenza, Laboratori Nazionali di Frascati; ^(b) Dipartimento di Fisica, Università della Calabria, Rende, Italy
- ⁴¹ ^(a) AGH University of Science and Technology, Faculty of Physics and Applied Computer Science, Krakow; ^(b) Marian Smoluchowski Institute of Physics, Jagiellonian University, Krakow, Poland
- ⁴² Institute of Nuclear Physics Polish Academy of Sciences, Krakow, Poland
- ⁴³ Physics Department, Southern Methodist University, Dallas TX, United States
- ⁴⁴ Physics Department, University of Texas at Dallas, Richardson TX, United States
- ⁴⁵ DESY, Hamburg and Zeuthen, Germany
- ⁴⁶ Lehrstuhl für Experimentelle Physik IV, Technische Universität Dortmund, Dortmund, Germany
- ⁴⁷ Institut für Kern- und Teilchenphysik, Technische Universität Dresden, Dresden, Germany
- ⁴⁸ Department of Physics, Duke University, Durham NC, United States
- ⁴⁹ SUPA - School of Physics and Astronomy, University of Edinburgh, Edinburgh, United Kingdom
- ⁵⁰ INFN e Laboratori Nazionali di Frascati, Frascati, Italy
- ⁵¹ Fakultät für Mathematik und Physik, Albert-Ludwigs-Universität, Freiburg, Germany
- ⁵² Département de Physique Nucléaire et Corpusculaire, Université de Genève, Geneva, Switzerland
- ⁵³ ^(a) INFN Sezione di Genova; ^(b) Dipartimento di Fisica, Università di Genova, Genova, Italy
- ⁵⁴ ^(a) E. Andronikashvili Institute of Physics, Iv. Javakishvili Tbilisi State University, Tbilisi; ^(b) High Energy Physics Institute, Tbilisi State University, Tbilisi, Georgia
- ⁵⁵ II Physikalisches Institut, Justus-Liebig-Universität Giessen, Giessen, Germany
- ⁵⁶ SUPA - School of Physics and Astronomy, University of Glasgow, Glasgow, United Kingdom
- ⁵⁷ II Physikalisches Institut, Georg-August-Universität, Göttingen, Germany
- ⁵⁸ Laboratoire de Physique Subatomique et de Cosmologie, Université Grenoble-Alpes, CNRS/IN2P3, Grenoble, France
- ⁵⁹ Laboratory for Particle Physics and Cosmology, Harvard University, Cambridge MA, United States
- ⁶⁰ ^(a) Kirchhoff-Institut für Physik, Ruprecht-Karls-Universität Heidelberg, Heidelberg; ^(b) Physikalisches Institut, Ruprecht-Karls-Universität Heidelberg, Heidelberg, Germany
- ⁶¹ Faculty of Applied Information Science, Hiroshima Institute of Technology, Hiroshima, Japan
- ⁶² ^(a) Department of Physics, The Chinese University of Hong Kong, Shatin, N.T.; ^(b) Department of Physics, The University of Hong Kong; ^(c) Department of Physics and Institute for Advanced Study, The Hong Kong University of Science and Technology, Clear Water Bay, Kowloon, Hong Kong, China
- ⁶³ Department of Physics, National Tsing Hua University, Taiwan
- ⁶⁴ Department of Physics, Indiana University, Bloomington IN, United States
- ⁶⁵ Institut für Astro- und Teilchenphysik, Leopold-Franzens-Universität, Innsbruck, Austria
- ⁶⁶ University of Iowa, Iowa City IA, United States
- ⁶⁷ Department of Physics and Astronomy, Iowa State University, Ames IA, United States
- ⁶⁸ Joint Institute for Nuclear Research, JINR Dubna, Dubna, Russia
- ⁶⁹ KEK, High Energy Accelerator Research Organization, Tsukuba, Japan
- ⁷⁰ Graduate School of Science, Kobe University, Kobe, Japan
- ⁷¹ Faculty of Science, Kyoto University, Kyoto, Japan
- ⁷² Kyoto University of Education, Kyoto, Japan
- ⁷³ Research Center for Advanced Particle Physics and Department of Physics, Kyushu University, Fukuoka, Japan
- ⁷⁴ Instituto de Física La Plata, Universidad Nacional de La Plata and CONICET, La Plata, Argentina
- ⁷⁵ Physics Department, Lancaster University, Lancaster, United Kingdom
- ⁷⁶ ^(a) INFN Sezione di Lecce; ^(b) Dipartimento di Matematica e Fisica, Università del Salento, Lecce, Italy
- ⁷⁷ Oliver Lodge Laboratory, University of Liverpool, Liverpool, United Kingdom
- ⁷⁸ Department of Experimental Particle Physics, Jožef Stefan Institute and Department of Physics, University of Ljubljana, Ljubljana, Slovenia
- ⁷⁹ School of Physics and Astronomy, Queen Mary University of London, London, United Kingdom
- ⁸⁰ Department of Physics, Royal Holloway University of London, Surrey, United Kingdom
- ⁸¹ Department of Physics and Astronomy, University College London, London, United Kingdom
- ⁸² Louisiana Tech University, Ruston LA, United States
- ⁸³ Laboratoire de Physique Nucléaire et de Hautes Energies, UPMC and Université Paris-Diderot and CNRS/IN2P3, Paris, France
- ⁸⁴ Fysiska institutionen, Lunds universitet, Lund, Sweden
- ⁸⁵ Departamento de Física Teórica C-15, Universidad Autónoma de Madrid, Madrid, Spain
- ⁸⁶ Institut für Physik, Universität Mainz, Mainz, Germany
- ⁸⁷ School of Physics and Astronomy, University of Manchester, Manchester, United Kingdom
- ⁸⁸ CPPM, Aix-Marseille Université and CNRS/IN2P3, Marseille, France
- ⁸⁹ Department of Physics, University of Massachusetts, Amherst MA, United States
- ⁹⁰ Department of Physics, McGill University, Montreal QC, Canada
- ⁹¹ School of Physics, University of Melbourne, Victoria, Australia
- ⁹² Department of Physics, The University of Michigan, Ann Arbor MI, United States
- ⁹³ Department of Physics and Astronomy, Michigan State University, East Lansing MI, United States
- ⁹⁴ ^(a) INFN Sezione di Milano; ^(b) Dipartimento di Fisica, Università di Milano, Milano, Italy
- ⁹⁵ B.I. Stepanov Institute of Physics, National Academy of Sciences of Belarus, Minsk, Belarus
- ⁹⁶ Research Institute for Nuclear Problems of Byelorussian State University, Minsk, Belarus
- ⁹⁷ Group of Particle Physics, University of Montreal, Montreal QC, Canada
- ⁹⁸ P.N. Lebedev Physical Institute of the Russian Academy of Sciences, Moscow, Russia
- ⁹⁹ Institute for Theoretical and Experimental Physics (ITEP), Moscow, Russia
- ¹⁰⁰ National Research Nuclear University MEPhI, Moscow, Russia
- ¹⁰¹ D.V. Skobeltsyn Institute of Nuclear Physics, M.V. Lomonosov Moscow State University, Moscow, Russia
- ¹⁰² Fakultät für Physik, Ludwig-Maximilians-Universität München, München, Germany
- ¹⁰³ Max-Planck-Institut für Physik (Werner-Heisenberg-Institut), München, Germany
- ¹⁰⁴ Nagasaki Institute of Applied Science, Nagasaki, Japan
- ¹⁰⁵ Graduate School of Science and Kobayashi-Maskawa Institute, Nagoya University, Nagoya, Japan
- ¹⁰⁶ ^(a) INFN Sezione di Napoli; ^(b) Dipartimento di Fisica, Università di Napoli, Napoli, Italy
- ¹⁰⁷ Department of Physics and Astronomy, University of New Mexico, Albuquerque NM, United States
- ¹⁰⁸ Institute for Mathematics, Astrophysics and Particle Physics, Radboud University Nijmegen/Nikhef, Nijmegen, Netherlands
- ¹⁰⁹ Nikhef National Institute for Subatomic Physics and University of Amsterdam, Amsterdam, Netherlands
- ¹¹⁰ Department of Physics, Northern Illinois University, DeKalb IL, United States
- ¹¹¹ Budker Institute of Nuclear Physics, SB RAS, Novosibirsk, Russia
- ¹¹² Department of Physics, New York University, New York NY, United States
- ¹¹³ Ohio State University, Columbus OH, United States
- ¹¹⁴ Faculty of Science, Okayama University, Okayama, Japan
- ¹¹⁵ Homer L. Dodge Department of Physics and Astronomy, University of Oklahoma, Norman OK, United States
- ¹¹⁶ Department of Physics, Oklahoma State University, Stillwater OK, United States

- 117 Palacký University, RCPTM, Olomouc, Czech Republic
 118 Center for High Energy Physics, University of Oregon, Eugene OR, United States
 119 LAL, Univ. Paris-Sud, CNRS/IN2P3, Université Paris-Saclay, Orsay, France
 120 Graduate School of Science, Osaka University, Osaka, Japan
 121 Department of Physics, University of Oslo, Oslo, Norway
 122 Department of Physics, Oxford University, Oxford, United Kingdom
 123 ^(a) INFN Sezione di Pavia; ^(b) Dipartimento di Fisica, Università di Pavia, Pavia, Italy
 124 Department of Physics, University of Pennsylvania, Philadelphia PA, United States
 125 National Research Centre “Kurchatov Institute” B.P. Konstantinov Petersburg Nuclear Physics Institute, St. Petersburg, Russia
 126 ^(a) INFN Sezione di Pisa; ^(b) Dipartimento di Fisica E. Fermi, Università di Pisa, Pisa, Italy
 127 Department of Physics and Astronomy, University of Pittsburgh, Pittsburgh PA, United States
 128 ^(a) Laboratório de Instrumentação e Física Experimental de Partículas - LIP, Lisboa; ^(b) Faculdade de Ciências, Universidade de Lisboa, Lisboa; ^(c) Department of Physics, University of Coimbra, Coimbra; ^(d) Centro de Física Nuclear da Universidade de Lisboa, Lisboa; ^(e) Departamento de Física, Universidade do Minho, Braga; ^(f) Departamento de Física Teórica y del Cosmos and CAFPE, Universidad de Granada, Granada; ^(g) Dep Física and CEFITEC of Faculdade de Ciências e Tecnologia, Universidade Nova de Lisboa, Caparica, Portugal
 129 Institute of Physics, Academy of Sciences of the Czech Republic, Praha, Czech Republic
 130 Czech Technical University in Prague, Praha, Czech Republic
 131 Charles University, Faculty of Mathematics and Physics, Prague, Czech Republic
 132 State Research Center Institute for High Energy Physics (Protvino), NRC KI, Russia
 133 Particle Physics Department, Rutherford Appleton Laboratory, Didcot, United Kingdom
 134 ^(a) INFN Sezione di Roma; ^(b) Dipartimento di Fisica, Sapienza Università di Roma, Roma, Italy
 135 ^(a) INFN Sezione di Roma Tor Vergata; ^(b) Dipartimento di Fisica, Università di Roma Tor Vergata, Roma, Italy
 136 ^(a) INFN Sezione di Roma Tre; ^(b) Dipartimento di Matematica e Fisica, Università Roma Tre, Roma, Italy
 137 ^(a) Faculté des Sciences Ain Chock, Réseau Universitaire de Physique des Hautes Energies - Université Hassan II, Casablanca; ^(b) Centre National de l'Energie des Sciences Techniques Nucleaires, Rabat; ^(c) Faculté des Sciences Semlalia, Université Cadi Ayyad, LPHEA-Marrakech; ^(d) Faculté des Sciences, Université Mohamed Premier and LPTPM, Oujda; ^(e) Faculté des sciences, Université Mohammed V, Rabat, Morocco
 138 DSM/IRFU (Institut de Recherches sur les Lois Fondamentales de l'Univers), CEA Saclay (Commissariat à l'Energie Atomique et aux Energies Alternatives), Gif-sur-Yvette, France
 139 Santa Cruz Institute for Particle Physics, University of California Santa Cruz, Santa Cruz CA, United States
 140 Department of Physics, University of Washington, Seattle WA, United States
 141 Department of Physics and Astronomy, University of Sheffield, Sheffield, United Kingdom
 142 Department of Physics, Shinshu University, Nagano, Japan
 143 Department Physik, Universität Siegen, Siegen, Germany
 144 Department of Physics, Simon Fraser University, Burnaby BC, Canada
 145 SLAC National Accelerator Laboratory, Stanford CA, United States
 146 ^(a) Faculty of Mathematics, Physics & Informatics, Comenius University, Bratislava; ^(b) Department of Subnuclear Physics, Institute of Experimental Physics of the Slovak Academy of Sciences, Kosice, Slovak Republic
 147 ^(a) Department of Physics, University of Cape Town, Cape Town; ^(b) Department of Physics, University of Johannesburg, Johannesburg; ^(c) School of Physics, University of the Witwatersrand, Johannesburg, South Africa
 148 ^(a) Department of Physics, Stockholm University; ^(b) The Oskar Klein Centre, Stockholm, Sweden
 149 Physics Department, Royal Institute of Technology, Stockholm, Sweden
 150 Departments of Physics & Astronomy and Chemistry, Stony Brook University, Stony Brook NY, United States
 151 Department of Physics and Astronomy, University of Sussex, Brighton, United Kingdom
 152 School of Physics, University of Sydney, Sydney, Australia
 153 Institute of Physics, Academia Sinica, Taipei, Taiwan
 154 Department of Physics, Technion: Israel Institute of Technology, Haifa, Israel
 155 Raymond and Beverly Sackler School of Physics and Astronomy, Tel Aviv University, Tel Aviv, Israel
 156 Department of Physics, Aristotle University of Thessaloniki, Thessaloniki, Greece
 157 International Center for Elementary Particle Physics and Department of Physics, The University of Tokyo, Tokyo, Japan
 158 Graduate School of Science and Technology, Tokyo Metropolitan University, Tokyo, Japan
 159 Department of Physics, Tokyo Institute of Technology, Tokyo, Japan
 160 Tomsk State University, Tomsk, Russia
 161 Department of Physics, University of Toronto, Toronto ON, Canada
 162 ^(a) INFN-TIFPA; ^(b) University of Trento, Trento, Italy
 163 ^(a) TRIUMF, Vancouver BC; ^(b) Department of Physics and Astronomy, York University, Toronto ON, Canada
 164 Faculty of Pure and Applied Sciences, and Center for Integrated Research in Fundamental Science and Engineering, University of Tsukuba, Tsukuba, Japan
 165 Department of Physics and Astronomy, Tufts University, Medford MA, United States
 166 Department of Physics and Astronomy, University of California Irvine, Irvine CA, United States
 167 ^(a) INFN Gruppo Collegato di Udine, Sezione di Trieste, Udine; ^(b) ICTP, Trieste; ^(c) Dipartimento di Chimica, Fisica e Ambiente, Università di Udine, Udine, Italy
 168 Department of Physics and Astronomy, University of Uppsala, Uppsala, Sweden
 169 Department of Physics, University of Illinois, Urbana IL, United States
 170 Instituto de Física Corpuscular (IFIC), Centro Mixto Universidad de Valencia - CSIC, Spain
 171 Department of Physics, University of British Columbia, Vancouver BC, Canada
 172 Department of Physics and Astronomy, University of Victoria, Victoria BC, Canada
 173 Department of Physics, University of Warwick, Coventry, United Kingdom
 174 Waseda University, Tokyo, Japan
 175 Department of Particle Physics, The Weizmann Institute of Science, Rehovot, Israel
 176 Department of Physics, University of Wisconsin, Madison WI, United States
 177 Fakultät für Physik und Astronomie, Julius-Maximilians-Universität, Würzburg, Germany
 178 Fakultät für Mathematik und Naturwissenschaften, Fachgruppe Physik, Bergische Universität Wuppertal, Wuppertal, Germany
 179 Department of Physics, Yale University, New Haven CT, United States
 180 Yerevan Physics Institute, Yerevan, Armenia
 181 Centre de Calcul de l'Institut National de Physique Nucléaire et de Physique des Particules (IN2P3), Villeurbanne, France
 182 Academia Sinica Grid Computing, Institute of Physics, Academia Sinica, Taipei, Taiwan

^a Also at Department of Physics, King's College London, London, United Kingdom.

^b Also at Institute of Physics, Azerbaijan Academy of Sciences, Baku, Azerbaijan.

^c Also at Novosibirsk State University, Novosibirsk, Russia.

^d Also at TRIUMF, Vancouver BC, Canada.

^e Also at Department of Physics & Astronomy, University of Louisville, Louisville, KY, United States of America.

- ^f Also at Physics Department, An-Najah National University, Nablus, Palestine.
- ^g Also at Department of Physics, California State University, Fresno, CA, United States of America.
- ^h Also at Department of Physics, University of Fribourg, Fribourg, Switzerland.
- ⁱ Also at II Physikalisches Institut, Georg-August-Universität, Göttingen, Germany.
- ^j Also at Departament de Física de la Universitat Autònoma de Barcelona, Barcelona, Spain.
- ^k Also at Departamento de Física e Astronomia, Faculdade de Ciências, Universidade do Porto, Portugal.
- ^l Also at Tomsk State University, Tomsk, Russia.
- ^m Also at The Collaborative Innovation Center of Quantum Matter (CICQM), Beijing, China.
- ⁿ Also at Università di Napoli Parthenope, Napoli, Italy.
- ^o Also at Institute of Particle Physics (IPP), Canada.
- ^p Also at Horia Hulubei National Institute of Physics and Nuclear Engineering, Bucharest, Romania.
- ^q Also at Department of Physics, St. Petersburg State Polytechnical University, St. Petersburg, Russia.
- ^r Also at Borough of Manhattan Community College, City University of New York, New York City, United States of America.
- ^s Also at Department of Financial and Management Engineering, University of the Aegean, Chios, Greece.
- ^t Also at Centre for High Performance Computing, CSIR Campus, Rosebank, Cape Town, South Africa.
- ^u Also at Louisiana Tech University, Ruston LA, United States of America.
- ^v Also at Institutio Catalana de Recerca i Estudis Avancats, ICREA, Barcelona, Spain.
- ^w Also at Graduate School of Science, Osaka University, Osaka, Japan.
- ^x Also at Fakultät für Mathematik und Physik, Albert-Ludwigs-Universität, Freiburg, Germany.
- ^y Also at Institute for Mathematics, Astrophysics and Particle Physics, Radboud University Nijmegen/Nikhef, Nijmegen, Netherlands.
- ^z Also at Department of Physics, The University of Texas at Austin, Austin TX, United States of America.
- ^{aa} Also at Institute of Theoretical Physics, Ilia State University, Tbilisi, Georgia.
- ^{ab} Also at CERN, Geneva, Switzerland.
- ^{ac} Also at Georgian Technical University (GTU), Tbilisi, Georgia.
- ^{ad} Also at Ochanai Academic Production, Ochanomizu University, Tokyo, Japan.
- ^{ae} Also at Manhattan College, New York NY, United States of America.
- ^{af} Also at Departamento de Física, Pontificia Universidad Católica de Chile, Santiago, Chile.
- ^{ag} Also at Department of Physics, The University of Michigan, Ann Arbor MI, United States of America.
- ^{ah} Also at The City College of New York, New York NY, United States of America.
- ^{ai} Also at Departamento de Física Teórica y del Cosmos and CAFPE, Universidad de Granada, Granada, Portugal.
- ^{aj} Also at Department of Physics, California State University, Sacramento CA, United States of America.
- ^{ak} Also at Moscow Institute of Physics and Technology State University, Dolgoprudny, Russia.
- ^{al} Also at Departement de Physique Nucleaire et Corpusculaire, Université de Genève, Geneva, Switzerland.
- ^{am} Also at Institut de Física d'Altes Energies (IFAE), The Barcelona Institute of Science and Technology, Barcelona, Spain.
- ^{an} Also at School of Physics, Sun Yat-sen University, Guangzhou, China.
- ^{ao} Also at Institute for Nuclear Research and Nuclear Energy (INRNE) of the Bulgarian Academy of Sciences, Sofia, Bulgaria.
- ^{ap} Also at Faculty of Physics, M.V. Lomonosov Moscow State University, Moscow, Russia.
- ^{aq} Also at National Research Nuclear University MEPhI, Moscow, Russia.
- ^{ar} Also at Department of Physics, Stanford University, Stanford CA, United States of America.
- ^{as} Also at Institute for Particle and Nuclear Physics, Wigner Research Centre for Physics, Budapest, Hungary.
- ^{at} Also at Giresun University, Faculty of Engineering, Turkey.
- ^{au} Also at CPPM, Aix-Marseille Université and CNRS/IN2P3, Marseille, France.
- ^{av} Also at Department of Physics, Nanjing University, Jiangsu, China.
- ^{aw} Also at University of Malaya, Department of Physics, Kuala Lumpur, Malaysia.
- ^{ax} Also at Institute of Physics, Academia Sinica, Taipei, Taiwan.
- ^{ay} Also at LAL, Univ. Paris-Sud, CNRS/IN2P3, Université Paris-Saclay, Orsay, France.
- ^{az} Also at PKU-CHEP.
- * Deceased.